DESIGN OF A DROPLET BASED MICROFLUIDIC REACTOR TO SYNTHESIZE CHITOSAN COATED IRON OXIDE NANOPARTICLES

A THESIS SUBMITTED TO

THE GRADUATE SCHOOL OF ENGINEERING AND SCIENCE

OF BİLKENT UNIVERSITY

IN PARTIAL FULFILLMENT OF THE REQUIREMENTS FOR

THE DEGREE OF

MASTER OF SCIENCE

IN

MECHANICAL ENGINEERING

By

Malik Abdul Wahab

June 2019

DESIGN OF A DROPLET BASED MICROFLUIDIC REACTOR
TO SYNTHESIZE CHITOSAN COATED IRON OXIDE NANOPAR-
TICLES

By Malik Abdul Wahab

June 2019

We certify that we have read this thesis and that in our opinion it is fully adequate, in scope and in quality, as a thesis for the degree of Master of Science.

_____
Emine Yegan Erdem(Advisor)

_____
Cağlar Elbüken

_____
Batur Ercan

Approved for the Graduate School of Engineering and Science:

_____
Ezhan Karaşan
Director of the Graduate School

ABSTRACT

DESIGN OF A DROPLET BASED MICROFLUIDIC REACTOR TO SYNTHESIZE CHITOSAN COATED IRON OXIDE NANOPARTICLES

Malik Abdul Wahab

M.S. in Mechanical Engineering

Advisor: Emine Yegan Erdem

June 2019

Nanoparticles possess unique structural, mechanical, thermal, optical and chemical properties which are highly dependent on their size; therefore it is important to be able to synthesize them uniformly. In general they are synthesized using conventional batch-wise techniques; however microfluidic platforms are also used because they provide precise control over reaction conditions like mixing time, temperature, concentration and improved reaction kinetics. This work is the first study where coating of magnetic nanoparticles with chitosan is realized by utilizing a microfluidic platform. These particles have potential application in targeted drug delivery due to their magnetic behavior and the possibility of carrying drug in the chitosan layer. In the past, this synthesis reaction was performed by using batch wise techniques. In this work we demonstrate the synthesis of chitosan coated nanoparticles using a droplet based microfluidic platform. PDMS devices are fabricated using conventional soft lithography technique. Droplets from two different reagents are generated using double T junction with tapered geometry. The taper angle is optimized such that both reagents generate droplets alternatively with efficiency of more than 95%. Viscosity and surface tension of both droplet phase and continuous phase is taken into account to optimize the geometry. As both reagents need to be mixed in equal proportion, flow rates are adjusted to make the spacing and size of droplets identical. Later, two consecutive droplets are merged in a pillar structure by using the fact that increasing the width of channel will slow down the droplets. Dimensions of channels are optimized so that only two consecutive droplets are merging while pillars avoid accumulation of droplets at that location. Olive oil and silicon oil are used as the continuous phase while chitosan solution and iron chloride solution are used as dispersed phases to form alternating droplets. Then ammonia solution is added as dispersed phase and it forms another droplet at a T-junction and this

droplet is merged with the upcoming droplet to initiate the reaction. Synthesized nanoparticles are characterized using transmission electron microscopy (TEM) and fourier-transform infrared spectroscopy (FTIR). As a side study, hydroxyapatite nanoparticles were also synthesized using this droplet-based microfluidic system at various concentration of reactants and results are analyzed using SEM imaging.

ÖZET

KITOSAN KAPLI DEMIR-OKSIT NANOPARCACIK SENTEZLEYEN DAMLACIK BAZLI MIKROAKISKAN REAKTOR TASARIMI

Malik Abdul Wahab

Makine Mühendisliği, Yüksek Lisans

Tez Danışmanı: Emine Yegan Erdem

Haziran 2019

Nanoparçacıklar yapısal, mekanik, termal, optik ve kimyasal özellikleri bakımından oldukça avantajlı malzemeler olup bu özellikleri parçacıkların boyutlarına bağlı olarak değişmektedir. Bu nedenle bu malzemeleri bir örnek olarak üretebilmek önem taşımaktadır. Genellikle nanoparçacıklar geleneksel yöntemler ile makro boyutlardaki ekipmanlar kullanılarak sentezlenmektedir ve bu tekniklerde reaksiyon koşulları istenildiği gibi kontrol edilememektedir. Öte yandan mikroakışkan sistemler ile karışma süresi, sıcaklık, konsantrasyon gibi reaksiyon koşulları çok daha iyi kontrol edilmektedir. Bu tez ise mikroakışkan bir reaktörde kitosan kaplı manyetik nanoparçacıkların sentezlenmesi üzerine yapılmış ilk çalışmadır. Bu tez kapsamında sentezlenen nanoparçacıkların kitasan çeperi ilaç taşınmasına, manyetik özelliği ise ilacın hedeflenebilmesine yarayabilecek uygulamalar için önem taşımaktadır. Literatürde kitosan kaplı manyetik nanoparçacıkların üretimi geleneksel beherli yöntemler ile gerçekleştirilmiştir. Bu tez kapsamında ise bu sentez damlacık temelli, PDMS'ten yumuşak litografi yöntemi ile üretilmiş mikroakışkan bir sistemde yapılmıştır. Mikroakışkan sistem damlacık temelli olup iki farklı kanaldan gelen kimyasallardan sıra ile damlacıklar oluşturulmakta ve sonrasında ise birleştirilerek kanal içerisinde karıştırılmaktadır. Açılı kanal girişleri kullanılarak %95 seviyesinde bir tekrarlanabilirlik ile sıralı damlacık oluşturulmuştur. Damlacıklar her seferinde aynı oranda birleştirilmelidir, bu nedenle de kanal içi akışlar kontrol edilmiş ve damlacıkların boyut ve aralıklarının aynı olması sağlanmıştır. Damlacıklar sıralı olarak oluşturulduktan sonra sütunlu ve genişleyip daralan bir kanalda birleştirilmişlerdir. Sütunlu yapının boyutları damlaların birbirini yakalayacakları sağlayacak şekilde optimize edilmişti. Silikon yağı taşıyıcı akışkan olarak kullanılmışı damlalar ise kitosan ve

demir klorür çözeltilerinden oluşturulmuştur. Kanalın ilerleyen kısmında da önceden birleştirilmiş damlalara amonyum çözeltisi eklenerek reaksiyonun tamamlanması sağlanmıştır. Sentezlenen nanoparçacıklar daha sonra elektron mikroskobu ve FTIR sistemi ile karakterize edilmiştir. Bu tez kapsamında son olarak bir yan çalışma da hirdoksiapetit nanoparçacıklarının yine aynı system kullanılarak sentezlenmesi ile yapılmıştır. Buradaki sonuçlar da taramalı electron mikroskobu ile incelenmiştir.

Anahtar sözcükler: Mikroakışkanlar, Nanoparçacıklar, sıralı damlacık ,birleştirilmiş damlalar, kompozit nanoparçacıklar..

Acknowledgement

First of all, i would like to thank my advisor Dr. Yegan Erdem for giving me the opportunity to study at Bilkent University and her guidance and patience during my thesis and master's studies. I am grateful for her time and consideration during this time . I am also thankful to her patience for reviewing my articles, including this thesis, and financial support for the needs in the manner of research and the conferences. I would also like to thank the jury members Asst. Prof. Cağlar Elbüken and Asst.Prof. Batur Ercan for their patience and invaluable feedback during the preparation of this thesis.

I would like to take this opportunity to thank the technical staff at UNAM specially Mr. Abdullah Kafadenk and Mr. Semih Bozkurt for their assistance with training of the equipment and for their help with the fabrication procedure for my microfluidic devices.

I would like to thank my group members Arsalan Nikdoost, Muhammad Saqib, Eliza Sopubekova, Ecem Yelekli , Gökçe Özkazanç, Mayssam Naji, Büşra Sarıarslan and Osaman Berkay Şahinoğlu for their help and support during exepriemnts. I would like to give special thanks to Asst. Prof Güneş Kibar for her support and help in experiments. I am grateful to Dr Azade Yelten and Asst. Prof. Batur Ercan for their collaboration in hydroxyapatite research.

I would like to acknowledge to my valuable friends Oğuz Altunkaş, Alper Topuz, Atakan Atay, Tamer Taşkıran, Kaan Karaca, Rico Morasata for their moral support during this time.

Last but not the least, I would like to acknowledge my family; my parents and my brother Usama, for their support and encouragements in every step of my life.

Contents

List of Figures

List of Tables

Chapter 1

Introduction

Nanoparticles have been the focus of researchers in the past few decades because of their unique structural, mechanical, thermal, optical and chemical properties [2]. Submicron level size of nanoparticles makes them very attractive for various applications like gene and drug delivery, [3, 4] detection of pathogens and proteins, [5, 6] studying of DNA [6] and separation of biological materials [7]. Most of these applications are influenced by the properties of nanoparticles that depend on their size; which clearly shows why it is so important to control the size of nanoparticles.

Nanoparticles have been synthesized by using conventional batch-wise methods for decades now. On the other hand recent advances in microfluidics have demonstrated several advantages over conventional batch-wise synthesis techniques such as high surface area to volume ratio and efficiency in mass and heat transfer at small scale. Microfluidic devices provide monodisperse nanoparticles due to having greater control over reaction kinetics, temperature, mixing and residence time [8, 9, 10]. Thus microfluidic reactors are advantageous as they provide high efficiency and accuracy as well as flexibility for multi step process, high throughput, reduction in sample usage and reduced exposure to toxic materials [11].

1.1 Flow Types in Microfluidic System

Microfluidic systems can be broadly classified into two categories on the basis of flow types: Continuous flow and segmented or droplet based flow. Flows are predominantly laminar in both of the cases; however depending on applications they become more useful than the others.

1.1.1 Continuous Flow System

Continuous flow systems have a single fluid flowing in channels. The flow is usually driven by pressure gradient. The fully developed flow has a parabolic velocity profile with zero velocity at the walls and maximum at the center of the channel. Zero velocity at the walls is governed by no slip at walls. Due to the non uniform velocity profile there is dispersion in the channels and fluid experiences different residence time depending on the location from the center line, thereby rendering this flow type unsuitable for nanoparticle synthesis or in some cases even biological applications. Moreover the synthesized nanoparticles may stick to the walls of channels causing clogging. Figure 1.1 shows the velocity profile inside the channel.
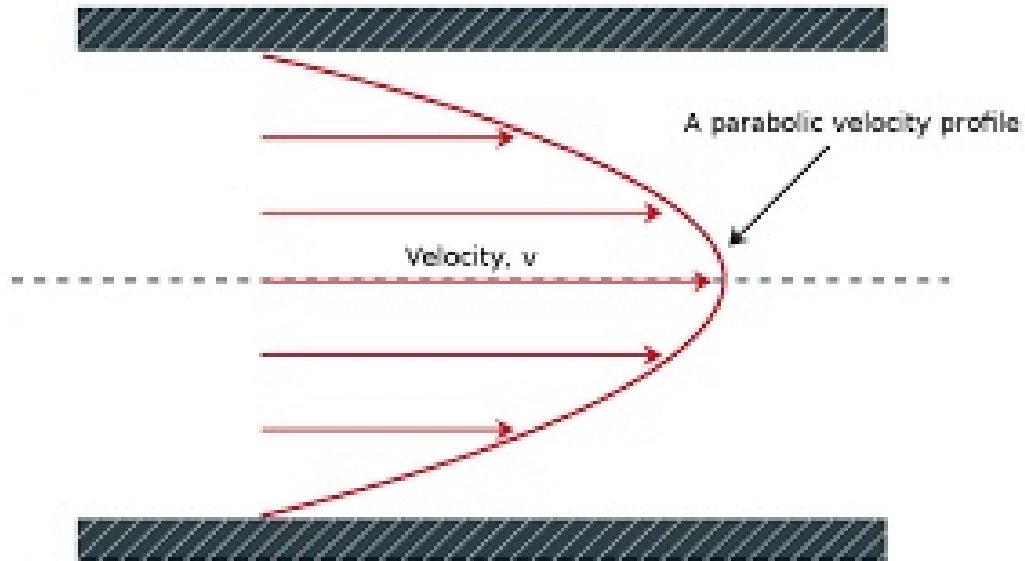
Figure 1.1: Velocity distribution inside a channel

1.1.2 Droplet Based Flow System

In case of a segmented flow or droplet based flow there exist two immiscible fluids. The fluid that wets the channel walls and carries the droplets is called as continuous phase or carrier fluid. Dispersed phase is carried in form droplets by the carrier fluid. The velocity of the droplet is uniform and there is no dispersion so the residence time is uniform for all of them. Moreover the droplets are surrounded by the continuous flow and there is no contact with the channel walls which eliminates the clogging problem. Mixing within the droplets is also enhanced by the circulation of fluid particles in droplet as shown in figure 1.2. These all factors count to narrow size distribution as compared to continuous flow systems.
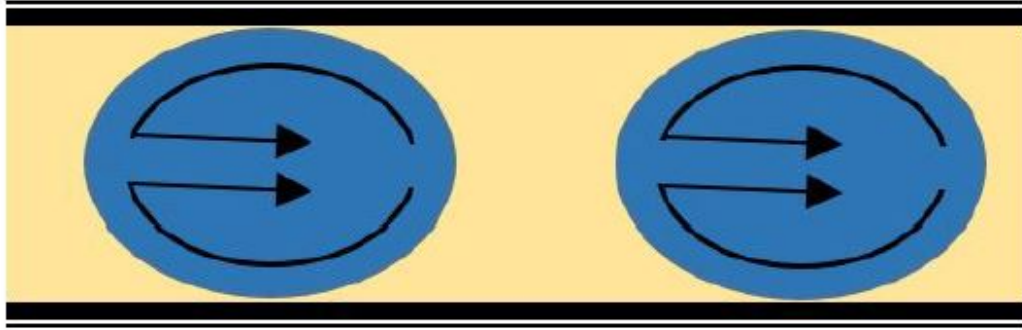
Figure 1.2: Flow profile in droplet based microfluidic reactor

T-junction and co-flowing designs are two most commonly used geometries to generate droplets. [12, 13, 14, 15, 16, 17, 18]

Droplet generation and size and spacing of droplets depends on geometry, properties of fluids and flow conditions like flow rate and flow rate ratio.

1.1.2.1 Governing parameters in droplet generation

Fluid behaviour can be explained in terms of dimensionless numbers. In the case of microfluidics Reynolds's number is always low which means that inertial effects are less dominant and surface forces, i.e viscous forces in this case, play a vital role. Secondly the Webber number which is a ratio of inertial force to surface tension would also be very small in microfluidics. Gravitational effects are also negligible which can be explained by the Bond number being less than 1, ratio of gravitational force to surface tension. Above discussion leaves surface tension and viscous forces to be the major forces in microfluidics. Capillary number gives the ratio between these two. Capillary number is given by equation 1.1.

$$Ca = \frac{\mu U L}{\gamma} \tag{1.1}$$

Where μ is the larger viscosity and γ is the the inter-facial surface tension. In case of low Ca number, surface tension forces dominate and spherical droplets are produced to minimize energy but in case of higher Ca number the viscous forces

are dominant and large deformations are observed resulting in droplets having asymmetric shapes or not forming at all

1.2   Microreactors for nanoparticle synthesis

Microreactors have been used for synthesizing nanoparticles for more than a decade now. The reason for utilizing microfluidic platform is the possibility to achieve monodisperse size distribution due to precise control over reaction conditions and residence time as explained earlier.

Semiconductor nanoparticles caught the attention of scientists quite early on because of their unique properties and applications. Shestopalov et al. used PDMS based device to synthesize CdS and CdS/CdSe nanoparticles using a multistep process [19]. A droplet based microreactor was used and reagents were mixed by using serpentine channels and conditions for merging of aqueous droplets were characterized using different capillary numbers. Hung et al. synthesized CdS nanoparticles using alternating droplet generation and controlled fusion of droplets in PDMS based microreactor and the size of nanoparticles was ranging from 4.2 nm to 8.2 nm [20]. Chan et al. developed a glass droplet based microreactor for high temperature synthesis of CdSe nanoparticles [21]. In the microreactor alternatingly formed reagents droplets were merged using nozzle geometry and later mixed in serpentine channels and resultant particles were monodisperse with average size of 3.5 nm . Yen et al. reported high temperature synthesis of CdSe quantum dots using multi zone silicon based microreactor [22].

Bio-materials have wide applications like drug delivery, biosensors, chromatography separation and information storage, due to which bio-compatible polymer nanoparticles have also been synthesized using microfluidic platforms. Sugiura et al. used a PDMS based microreactor to synthesize calcium alginate gel microparticles [23]. Particles were synthesized and later combined to get composite particles in a microfluidic chip. Zhang et al. reported synthesis of bio-polymer hydrogel particles using PDMS microreactor and by varying residence time various

shapes of hydrogel particles were obtained [24].

Song et al. reported the synthesis of paladium nanopaticles using a PEEK (polyetheretherketone) substrate [25]. Microreactor had 5 parallel reactors, each reactor containing 4 way mixers and three way reaction channels. Both batch-wise synthesis and microfluidic synthesis were performed and compared and it was concluded that nanoparticles from microreactor had narrower size distribution. Synthesis of copper nanoparticles using a similar microreactor was also reported [26]. Le et al. synthesized silver nanoparticles using a microreactor composed of micro-channels fabricated from stainless steel and immersed in oil bath for continuous and constant heating [27].

Gold nanoparticles were synthesized by J. M. Köhler using microfluidic channels, using etching to produce micro channels in silicon and then bonding to pyrex glass for optical access [28]. J. M. Köhler also used microfluidic devices with channels in pyrex glass and then bonding with silicon to enclose the channels [29, 30]. Both of these devices employed continuous flow and resulted in narrower size distribution as compared to conventional batch-wise synthesis. Erdem et al. reported a multi temperature zone droplet based microreactor for synthesis of titanium dioxide nanoparticles at high temperature and synthesized titanium oxide nanoparticles at different temperatures with an average size of 26.5 nm [31].

1.3   Synthesis of Iron Oxide Nanoparticles

Synthesis of magnetic iron oxide nanoparticles has attracted a lot of attention in past because of their applications in various fields like bioimaging, [32, 33] drug delivery, [34] magnetic data storage, [35] hyperthermia, [36] and separation of biological samples [37] .

1.3.1 Batch-wise Synthesis of Iron Oxide Nanoparticles

Synthesis of iron oxide nanoparticles has been going on for a long time because of their remarkable properties and applications. The most common method for synthesizing iron oxide nanoparticles is co-precipitation. Fe(II) and Fe(III) salts are mixed in presence of a basic solution either at room temperature or at high temperature. Babes et al. used chloride salts and tetramethylammonium hydroxide (TMAOH) to synthesise iron oxide nanoparticles for MRI contrast study [38]. Park et al. used entacarbonyliron and oleic acid in different moralities to produce nanoparticles with various size ranging from 6 to 15 nm [39]. Maity et al used chloride salts and ammonium hydroxide to synthesize magnetic nanoparticles and stabilized in aqueous solution of dodecane and kerosene and also by producing a stabilizing coating using oleic acid [40].

1.3.2 Microfluidic Synthesis of Iron Oxide Nanoparticles

Synthesis of nanoparticles using microfluidic system has advantages over conventional techniques like monodisperse size distribution, which is why there has been a shift from conventional techniques to microfluidic systems.The reason for preferring microfluidic platforms is due to their ability to control reaction conditions and residence time as stated earlier. Frenz et al. synthesized iron oxide nanoparticles using droplet based microfluidic reactor [41]. Droplets from Fe(II) and Fe (III) chloride solution and ammonium hydroxide solution were generated using coupled nozzles and were merged using electrocoalescence and the nanoparticles obtained had high mondispersity with average size of 4 nm. Abou Hassan et al. used chloride salt and tetramethylammonium hydroxide in co axial continuous flow microfluidic device to synthesize iron oxide nanoparticles [42]. The resultant nanoparticles were supermagnetic and average diameter was 6 nm with standard deviation of 0.2. Abou hasan et al.reported mutistep process for synthesis of iron oxide nanoparticles and then its encapsulation in silica on a single microfluidic platform with overall average size of 50nm [43].

Zhang et al. employed a two step process to synthesize and coat iron oxide nanoparticles with ZIF-8 [44]. Kumar et al. reported synthesis of magnetic iron oxide core shell nanoparticles using a droplet based microreactor and utilized the nanoparticles for MRI and found quite high saturation magnetization [45]. Recently an open microfluidic platform was also used to synthesize iron oxide nanoparticles [46]. Textured surfaces were used to move droplets of reagents using vertical vibration and then both droplet were merged at a junction and continued down the track to synthesize iron oxide nanoparticles. This method eliminates the clogging issue faced in channels.

1.4 Synthesis of Chitosan Nanoparticles

Chitosan has been recently investigated as a biopolymer to be used as gene carrier [47] and for drug delivery. [48]

1.4.1 Batch-wise Synthesis of Chitosan Nanoparticles

Chitosan nanoparticles have been synthesized using conventional batch-wise techniques for quite some time now because of applications in protein, gene and drug delivery. Qi et al. prepared chitosan nanoparticles using gelation of chitosan with tripolyphosphate solution and investigated antibacterial activity of nanoparticles [49]. Janes et al. synthesized chitosan nanoparticles loaded with doxorubicin by mixing doxorubicin with chitosan solution and precipitating at pH of 5 [50].

Xu et al. synthesized chitosan nanoparticles, with diameter from 20 to 200 nm, in various formation using ionic gelation of chitosan with tripolyphosphate and investigated the effect of structure on protein delivery [51]. Katas et al. produced and used chitosan nanoparticles for gene delivery [52]. The size of nanoparticles was less than 500 nm depending on type, molecular weight as well as concentration of chitosan. Grenha et al. prepared microencapsulated chitosan nanoparticles and used for lung protein delivery. Nanoparticles were prepared

using ionotropic gelation of chitosan with tripolyphosphate (TPP) [53].

1.4.2 Microfluidic Synthesis of Chitosan Nanoparticles

The biological applications of chitosan nanoparticles require uniform size as well therefore it is very important to control the size distribution of nanoparticles. That is why there have been a shift from conventional methods to microfluidic platforms for the synthesis of chitosan nanoparticles. Majedi et al. [54] synthesized hydro-dynamically modified chitosan nanoparticles using continuous microfluidics and showed the self assembly of chitosan particles. Flow focusing device was used to precipitate chitosan in acidic pH with basic water used as a buffer solution. Encapsulation and drug release profile of anticancer drug was also investigated. Çetin et al. reported microfluidic device for the synthesis of chitosan nanoparticles using chitosan solution in acetic and tripolyphosphate (TPP) [55].

Yang et al. used a droplet based microfluidic reactor to synthesize monodisperse chitosan microparticles [56]. Emulsions of chitosan solutions were formed using T junction and then droplets were sorted according to their size. Larger and smaller droplets were gathered in two different reservoirs containing TPP solution where reaction took place and precipitate was collected. Lee et al. synthesized chitosan microfibers for bio-artificial liver chip [57]. A microfluidic platform was proposed to fabricate the microfibers with varying diameter and was then used for bio-artificial liver chip.

1.5 Synthesis of Composite Nanoparticles

Composite nanoparticles have attracted the attention of scientists because of their outstanding properties and applications in several fields. Another reason for exploring the synthesis of composite nanoparticles is that they show much different properties compared to plain particles [58]. Hence there is a possibility

of coming up with novel materials. Composite nanoparticles especially polymer-metal/metal oxides nanoparticles have attracted a lot of attention. Composite nanoparticles have been synthesized using batch-wise techniques for a long time but due to high monodispersity in size, control over reaction condition and residence time in the microfluidic platform, there have been a shift to microreactor for composite nanoparticle synthesis. Another reason for this shift is the multistep process for composite material synthesis. Conventional synthesis combine both these steps in one and thereby resulting in non homogeneous size but microreactors has the ability separate these steps which results in homogeneous size [59].

Wang et al. produced ZnS-coated CdSe composite particles using a microfluidic platform [60]. Size of nanoparticles was controlled by changing the residence time. Both precursors were mixed and heated to precipitate. Zhang et al. synthesized PDMS coated gold nano fibers and studied its properties and applications in protein immobilization,immunoassays and other biochemical analysis on PDMS microchips [61].Yang et al. synthesized silver-chitosan composite nanoparticles using a droplet-based microfluidic device [62]. Emulsions of solution of chitosan and silver nitrate were generated and then collected in sodium hydroxide bath and nanoparticles were collected. Antibacterial properties of these nanoparticles were studied which make them useful for potential applications such as bactericidal agents for water disinfection, anti-pathogens and surface plasma resonance enhancers.

Hwang et al. used a droplet based microfluidic platform to synthesize magnetic hydrogel microparticles [63]. PDMS based device were used to generate emulsions and were exposed to UV radiation to react by UV polymerization.Valencia et al. reported a microfluidic platform with hydrodynamic flow focusing to produce lipid-polymer and lipid-quantum dots in as single step [64]. Continuous flow microfluidic platform with serpentine channels for passive mixing. Polymer core can be used for drug encapsulation and quantum dot core for imaging application and shell is made of lipid in both cases.

1.5.1 Synthesis of Composite Nanoparticles (Iron-oxide coated with different materials)

Magnetic iron oxide nanoparticles have applications in fields like drug delivery [34], hyperthermic treatment [65], magnetic resonance imaging (MRI) [66] and selective separation of biological fluids [67]. Due to these applications iron oxide nanoparticles coated with different materials has been synthesized both using conventional techniques as well as microfluidic platform. In this section microfluidic synthesis will be discussed only.

Kumar et al. synthesized dextran coated super-magnetic iron oxide nanoparticles for MRI applications [45]. Droplet based microfluidic reactor was utilized and crystalline particles were obtained with mean diameter 3.6 nm and standard deviation 0.8 nm. Santra et al. synthesized used micro emulsions to synthesize silica coated iron oxide nanoparticles for various applications [68]. Effect of different surfactants and basic solutions on the size and structure of nanoparticles were also investigated and the mean diameter for different conditions varied between 3 and 9 nm with standard deviation of 1 to 4 nm. Abou-Hassan et al. used multi step reactor to coat iron oxide nanoparticles with silica [43]. Continuous flow microreactor was used and resultant particles had average size of 50 nm with one or more iron oxide nanoparticles in each. Rao et al. encapsulated iron oxide nanoparticles in erythrocyte using using electroporation in microfluidic device [69].

1.5.2 Synthesis of Chitosan Coated Iron oxide Nanoparticles

Magnetic properties of iron oxide and bio-compatibility of chitosan can be used together for targeted drug delivery. Most of drugs used in chemotherapy are detrimental to healthy cells as well as diseased cells, thereby causing many side effects like weakness, nausea etc which are quite painful. A key solution to deal

with this problem is targeted drug delivery, where a drug carrying agent is delivered to directly to the infected area and then releases the drug into infected cells.

Chitosan can be used in drug delivery due to its biocompatibility, low toxicity, biodegradability and stability. [70, 71] When it is synthesized in nanometer dimensions, due to its small size and pH responsive chemistry it can penetrate into cells to release the drug that it carries. [70]

Due to their small size, magnetic nanoparticles behave as single domain materials and therefore when there is an applied external magnetic field, they behave like a paramagnet. This effect is named as 'paramagnetism' which means that when there is a magnetic field, nanoparticles align themselves with the applied field. In order to perform targeted drug delivery, nanoparticles should be composed of both a magnetic material and chitosan that carries the drug.

Chitosan coated iron oxide nanoparticles has been synthesized before using batch-wise techniques for various applications. Unsoy et al. synthesized chitosan coated iron oxide nanoparticles by co-precipitation of Fe(II) and Fe(III) with chitosan solution [72]. Safari et al. used a similar procedure to obtain chitosan decorated iron oxide particles and used as catalyst in in the synthesis of phenytoin derivatives [73]. Zarnegar et al. reported the use of composite nanoparticles as catalyst for for the synthesis of 2, 4, 5-trisubstituted imidazoles [74]. He et al. described a single step and two step process for the synthesis of chitosan decorated iron-oxide nanoparticles and reported their performance for the removal of furfural from aqueous solution [75].

Overall the remarkable properties of chitosan coated iron-oxide nanoparticles makes them very suitable for various application especially targeted drug delivery. In bio medical applications the size of nanoparticles is very important. The size of nanoparticles should be small enough to avoid any issues in circulation and should not cause pulmonary embolism. [72] Hence monodispersity in size is required in order to use all the nanoparticles.

Microfluidic platform has been quite promising in giving a narrower size distribution. The reactor introduced in this thesis is the first attempt to synthesize chitosan coated iron oxide nanoparticles using a microfluidic platform to the best of our knowledge.

1.6   Thesis Overview:

In this thesis a droplet based microreactor that combines droplet generation, merging and mixing is designed and utilized to synthesize chitosan coated iron oxide nanoparticles. By this way a multi step reaction is performed in single reactor.

Chapter 2 describes the design and fabrication process for the microreactor. Detailed description of design process and optimization is given starting from preliminary design to the final design. Fabrication procedure of the devices is also described.

Chapter 3 introduces the batch wise synthesis of nanoparticles and then experiments regarding the microfluidic synthesis are described. Results from both type of synthesis are also presented.

Chapter 4 describes the use of the microreactor to synthesize other materials like hydroxyapatite using varying concentration of precursor solution. And a brief overview of results is presented.

Chapter 5 provides the summary and conclusion of thesis and gives recommendation for future work.

Chapter 2

Design and Fabrication of the Microfluidic reactor

Continuous flow and droplet based flow systems have been used to synthesize nanoparticles as described in chapter 1. Droplet based flow systems have advantages over continuous flow system such as uniform residence time, no dispersion and no contact with channels walls which eliminates clogging issue. Hence a droplet based microreactor has been to synthesize composite nanoparticles. Microreactor consist of three essential components integrated in single microfluidic chip, alternate droplet formation platform. merging platform and mixing platform. In this chapter a design and fabrication of the microreactor is presented.

2.1 Fabrication of the Microreactor

Different materials could be used to prepare microfluidic reactor. Polymers especially Polydimethylsiloxane (PDMS) is most commonly used for microlfuidic reactors. One of the main reason for using PDMS is the ease of fabrication process. It is easily fabricated using conventional soft photo-lithography. They are

cost effective but have a limitations regarding operating temperature and pressure. As the reactions were performed at room temperature so there was no issue of temperature in this case.

Figure 2.1 shows the fabrication steps of microreactor.
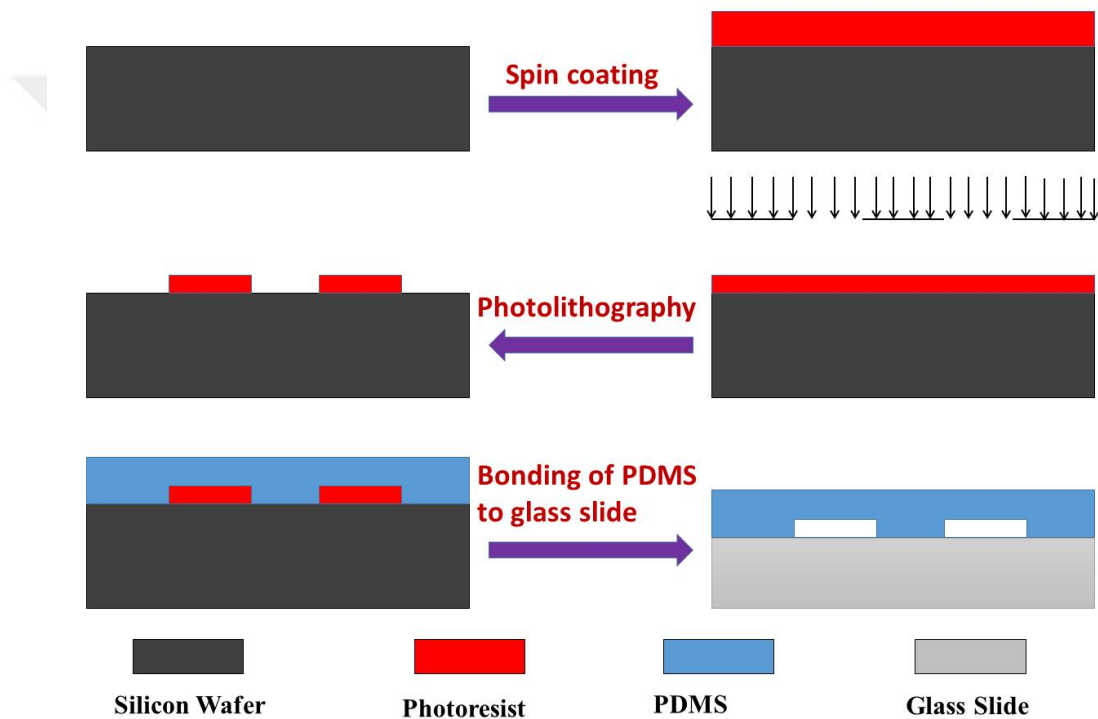
Figure 2.1: Photolithography fabrication steps for the PDMS microreactor

1) Firstly a silicon wafer is cleaned using acetone, isoproponal and water.

2) Then photo resist is coated by spin coating.

3) After the pre bake step photoresist is exposed to UV light through mask.

4) After the developement channels are formed on the silicon wafer.

5) PDMS and curing agent in the ratio of 10:1 are mixed, poured on silicon mold and cured.

6) After curing, PDMS is peeled off and bonded to glass slide to close the

channels.

Details of fabrication process and recipe can be found in Appendix A.

2.2 Design of the Microreactor

Microreactor design is an iterative process. In this section the whole process starting from initial design to the final design is presented.

2.2.1 Initial Design

Initially a simple design was proposed with three inlets for dispersed phase and one for continuous phase as presented in Figure 2.2.
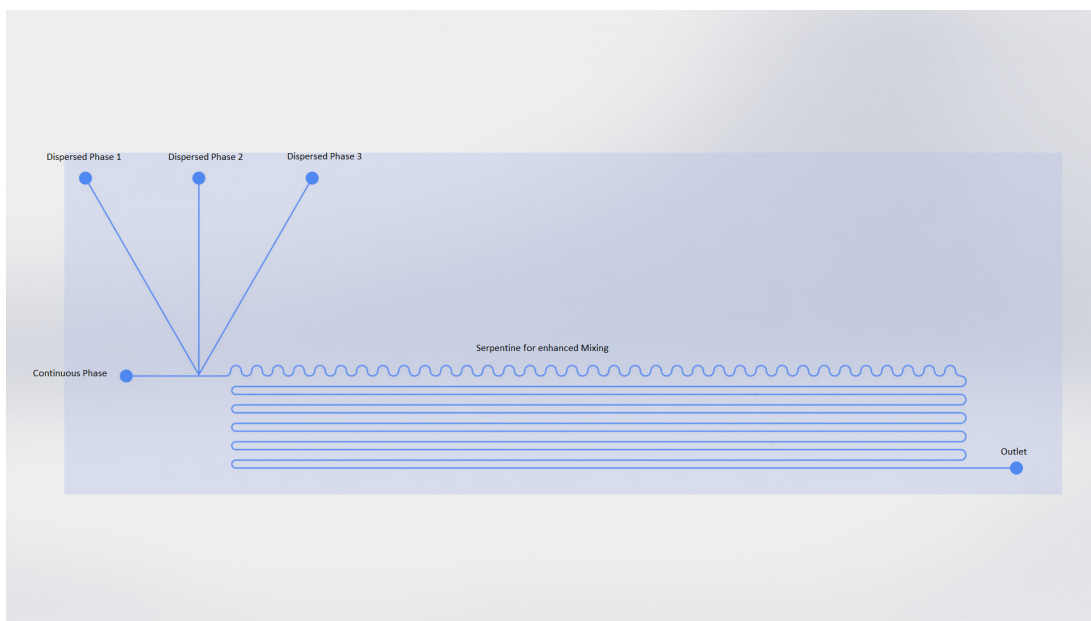
Figure 2.2: Layout of the initial Design

In this design the idea was to mix and form droplets out of three reagents required for the synthesis and to use olive oil as the continuous phase. A T-junction was used to form droplets and mix reagents inside the serpentine channels. After

mixing of the reagents the reaction would take place in the straight channels and nanoparticles were collected at the outlet. The channels were 100μm wide and the height was also 100μm.
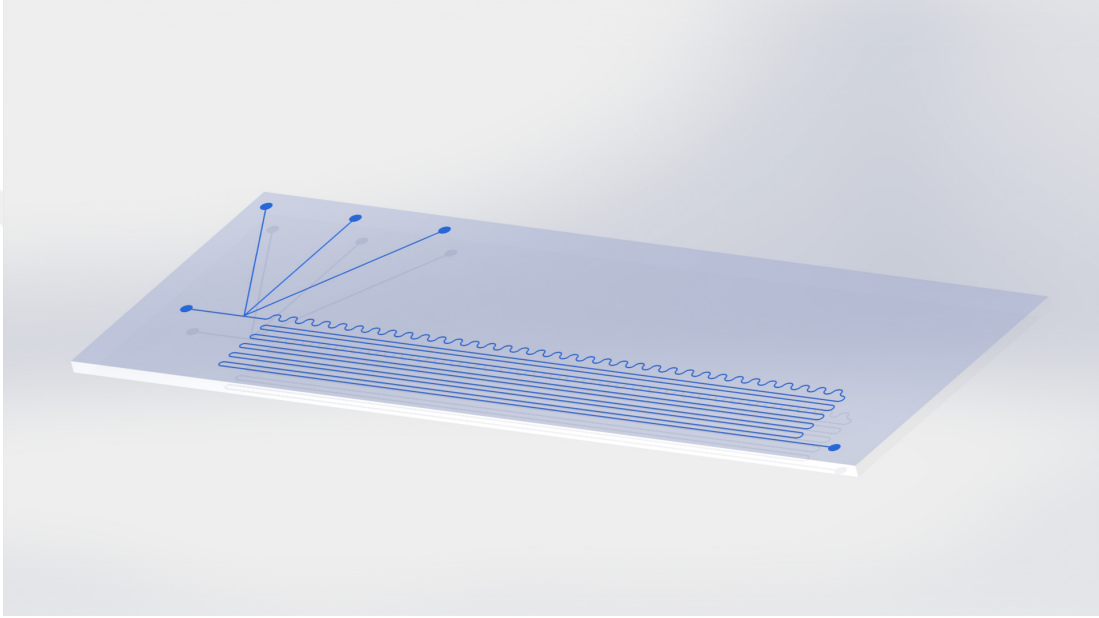
Figure 2.3: 3D View of initial design

However this design had a few issues. As the pressure in rectangular channels is given by the following equation.

$$\Delta P = \frac{12\mu L}{Wh^3}Q \tag{2.1}$$

Where μ is viscosity, L is the length of channel and W and h are dimensions of cross section W being larger than h and Q is the flow rate. As the length of channels were about 1 m, the pressure exerted to the inlets were quite high and PDMS could not hold that much pressure there by causing the leakage. And the reaction was so vigorous that the reagents were reacting before even forming the droplet and clogging the T junction and therefore disrupting the flow as shown in Figures 2.4 and 2.5. Due to these reasons, the design of microfluidic device was modified.
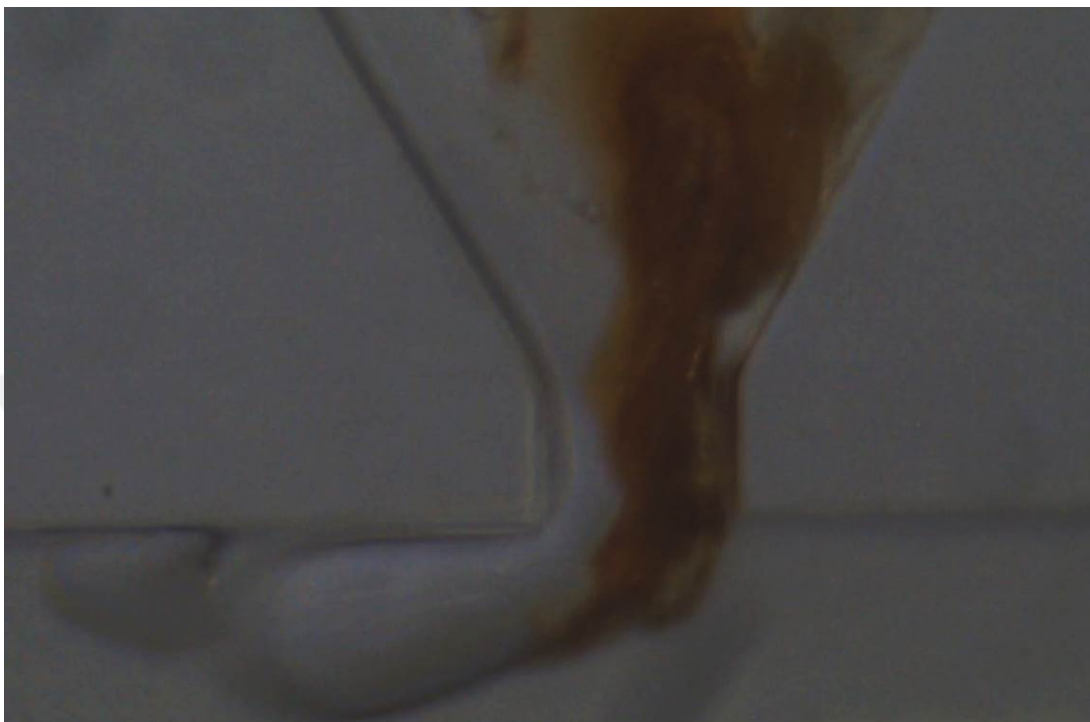
Figure 2.4: T-junction clogged due to vigorous reaction
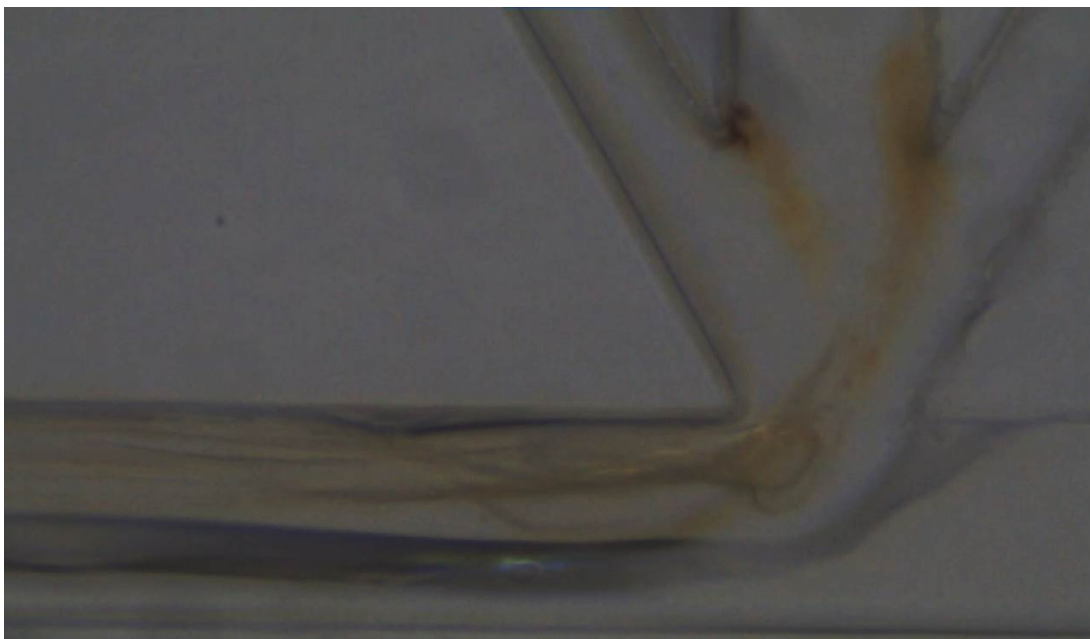
Figure 2.5: T-junction clogged due to vigorous reaction

2.2.2 Initial Improvisation in Design

After considering all those factors a new design was presented. As shown in Figure 2.6 separate T junctions were introduced to generate droplets from each reagents. The length of channels were also decreased to a considerable extent there by reducing the back pressure and eliminating the back flow. The channels were 100μm wide and the height was also 100μm.
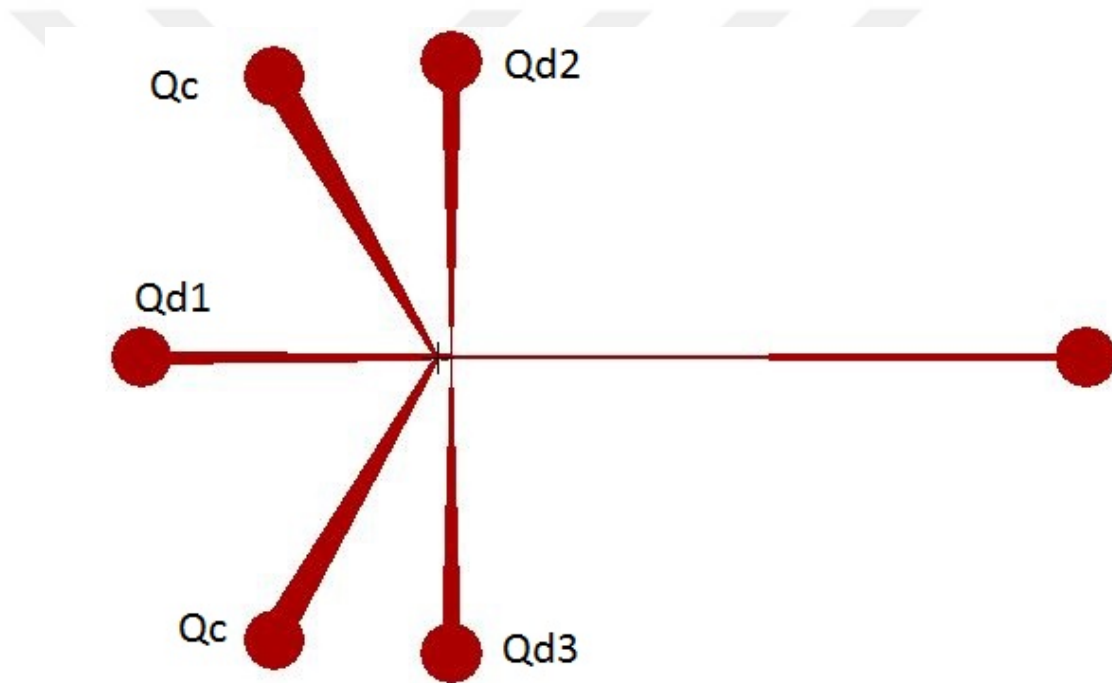
Figure 2.6: Layout of the device. Here Qc is continuous phase while Qd1, Qd2 and Qd3 are dispersed phase 1, 2 and 3 respectively

All the three dispersed phases were forming the droplets separately. Dispersed phase 2 and dispersed phase 3 were supposed to alternate in droplet formation while dispersed phase 1 droplet were to be merged with those to initiate reaction. But there was no clear pattern of alternation between droplets from dispersed phase 2 and dispersed phase 3. However underlying issue in this design was the merging of droplets. Droplets were not merging at the double T junction and hence it could not be concluded that the reaction was taking place in droplets as shown in Figure 2.7

Figure 2.7: Snapshot of experiment

2.2.3 Second Improvisation in Design

As there were two issues presented in the previous design, the following steps were taken to make sure there is an alternative droplet formation from two reagents and the droplets are merging.

2.2.3.1 Alternating Droplet Formation Geometry

Saqib et al. investigated different geometries for alternating droplet formation [76]. Tapered inlet channels were used for dispersed phase and angle for taper was modified to see the effect on the efficiency of droplet formation. It was concluded that a taper angle of 25° was very efficient for alternating droplet generation. Hence that geometry was employed to get alternating droplets from two reagents.

2.2.3.2 Merging of Droplets

After solving issue of alternating droplets, focus was on to find a solution to merge droplets efficiently. The concept behind this was the continuity equation.

$$Av = Constant \qquad (2.2)$$

where A is the cross section area of channels and v is the velocity of continuous phase. If area is increased the velocity will go down by same proportion. Hence by changing the width of channels, it is possible to slow down the two droplets such that they catch up on each other and merge.

A simple geometry possible was used to increase the width of channels to favour merging and then decreased the width to normal dimensions proposed and demonstrated by Bremond et al. [1] (Figure 2.8). However it is not stable for long times. Droplets may start accumulating in that region and more than two droplets may merge depending on the size of the droplets. And it will be quite difficult to make sure that only two droplets should merge and this goes on for the whole time the experiment is running.

In order to avoid accumulation of droplets in the extended section of channels, pillar induced geometry was proposed [77]. The physics behind this geometry is still the continuity equation, however pillar structures keep the droplets in straight line and avoid accumulation. The pillar structure is shown in Figure 2.9:

Both alternating droplet generation platform and pillar induced geometry was combined as shown in Figure 2.10. In this device tapered inlets generate droplets alternatively which are later merged in the pillar induced geometry and a third reagent droplet is also merged in the pillar induced geometry.

The issues faced in this device were related to merging of droplets from dispersed phase 1 with the merged droplet of dispersed phase 2 and 3. Apart from that some of the droplets were seen escaping through the side channels instead of going from the centre of pillars as seen in Figure 2.11. These issues were
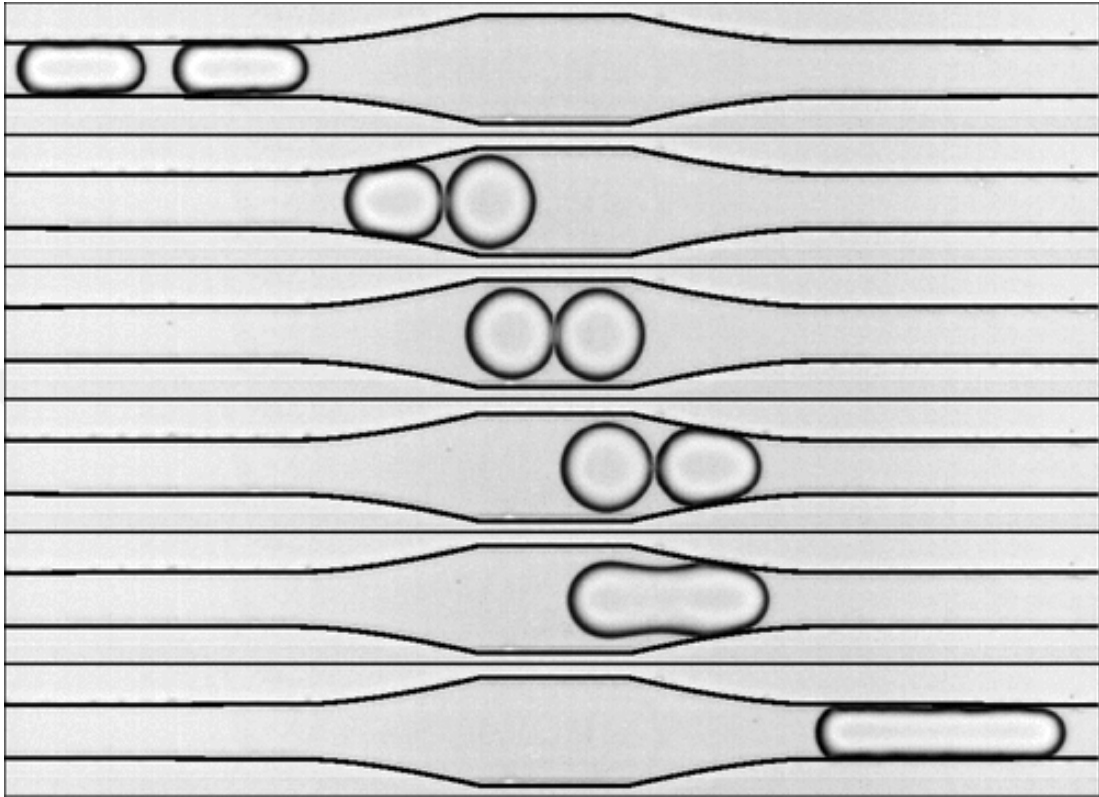
Figure 2.8: Time sequence showing the destabilization of a droplet pair passing through a symmetrical coalescence chamber: collision, relaxation, separation, and fusion. Reproduced with permission [1]

investigated experimentally and the solution is provided in next section

2.2.4   Final Design

In order to overcome the problem faced in previous design, a new approach was considered. In this approach first tapered geometry was used for alternate droplet generation which are then merged using pillar induced geometry. Merged droplet will then go undergo mixing in serpentine channels and finally the third reagent will be introduced from another inlet to initiate reaction. Mixing and reaction will occur in serpentine channels and nanoparticles will be collected from outlet. The schematic is shown in Figure 2.12. And the fabricated device is shown in Figure 2.13.
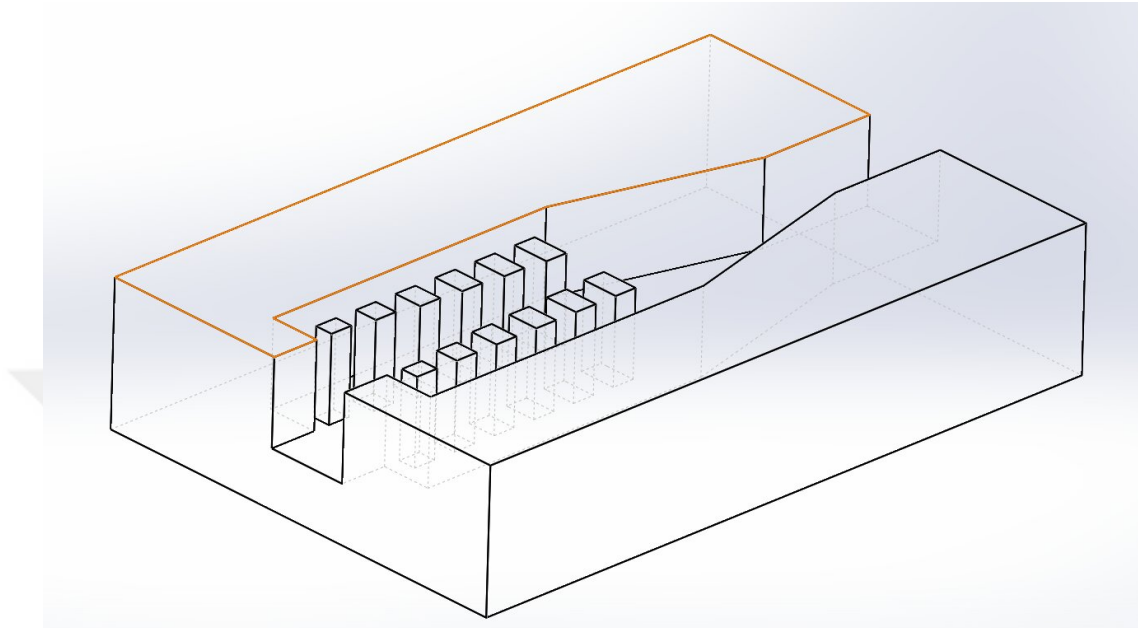
Figure 2.9: 3-D model of pillar structure
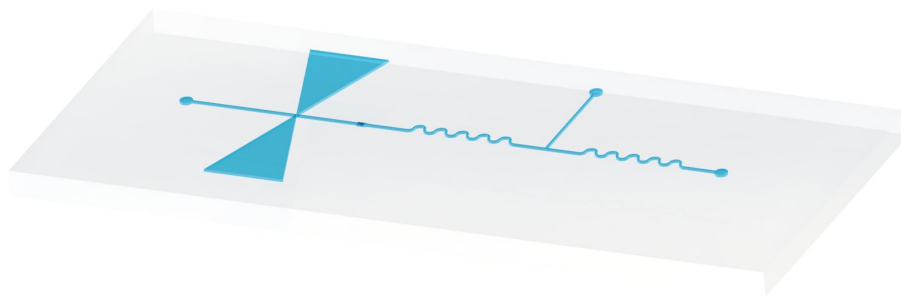
Figure 2.12: Lay out of the device with alternate droplet generation and merging geometry
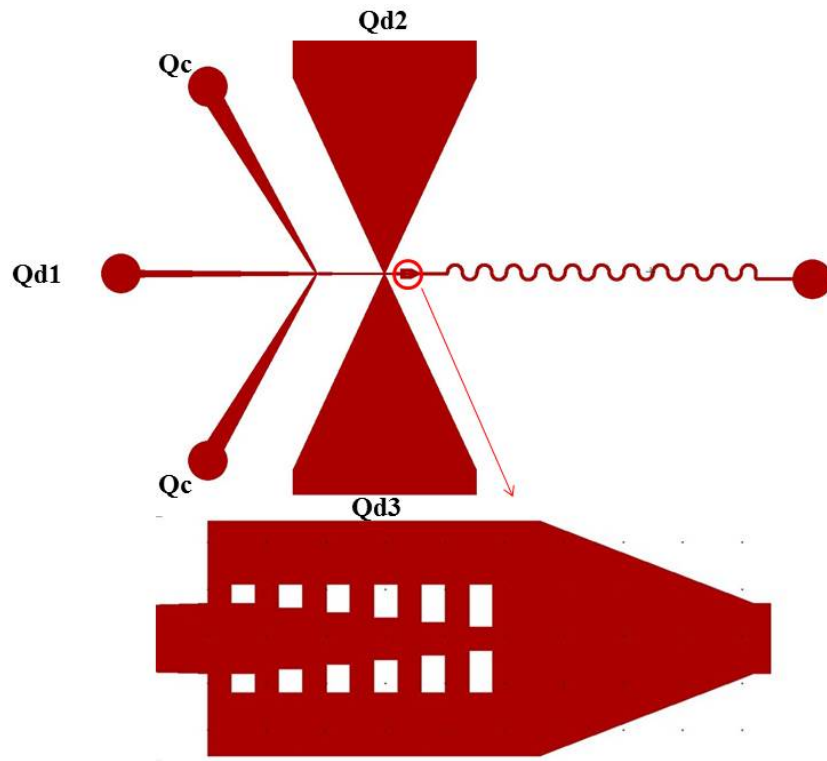
Figure 2.10: Layout of the device with alternating droplet generation and pillar induced merging geometry where Qc is continuous phase while Qd1, Qd2 and Qd3 are dispersed phase 1, 2 and 3 respectively

Figure 2.13: Fabricated device
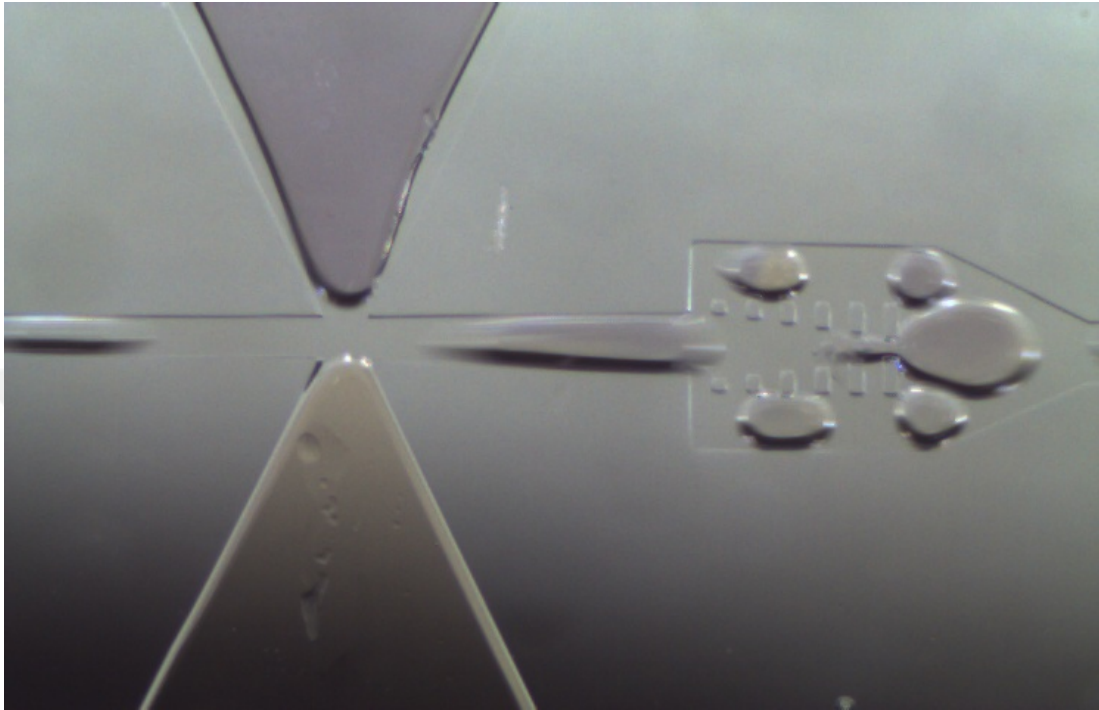
Figure 2.11: Experimental snapshot showing the droplet escaping from side channels

2.2.4.1 Optimization of Pillar induced merging geometry

Pillar induced merging geometry needed to be optimized in order for merging to take place at all the time and to prevent the side flow. If a part of droplet is escaping from sides it means that the concentration of reagent has changed and the reaction will not take place if the molarity of solution is different. Hence it was essential to optimize the dimensions. Three geometries were used as shown in Figure 2.14.
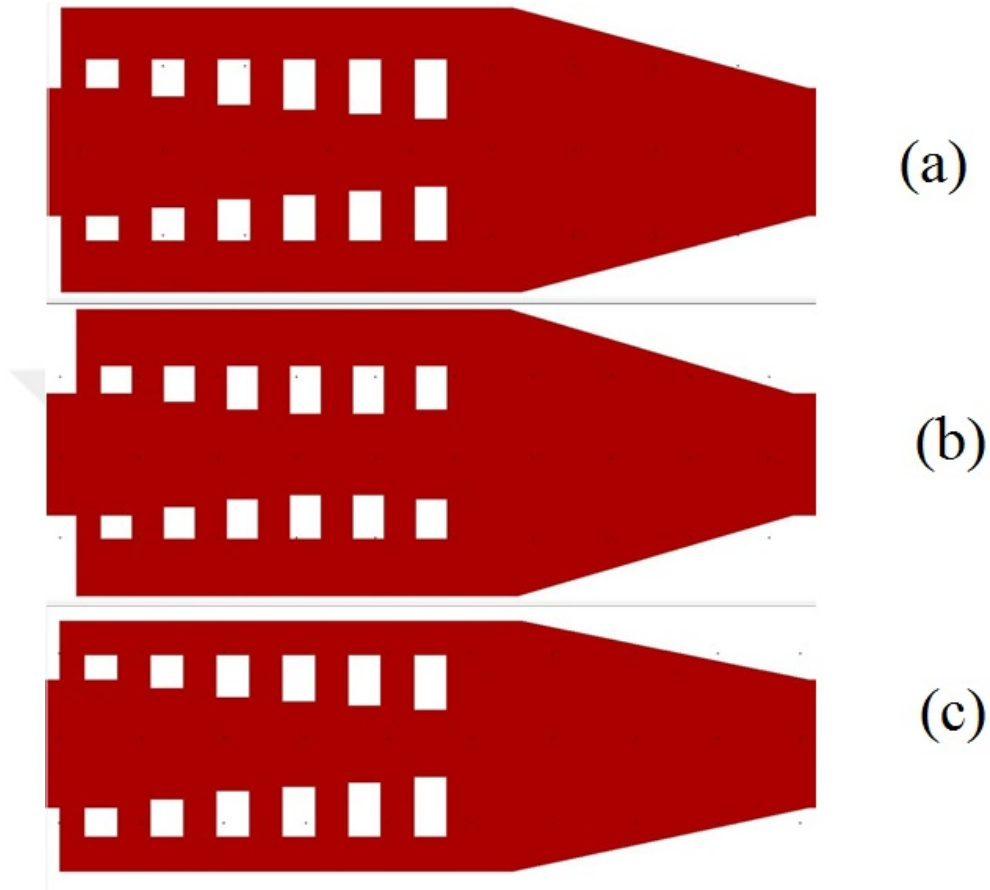
Figure 2.14: Pillars induced merging geometry with different widths (a) 335μm (b) 355μm (c) 250μm

In Figure 2.14 c,the width of 250 μm and dimensions of pillars are increasing downstream by 10 μm . However this was not enough for droplets to slow down and merge so the droplets escaped without merging at all.

In Figure 2.14 b the width is 355 μm and the width of pillars in increasing by 10 μmat first then start decreasing after fourth pillar by 5 μm. The droplets were merging in this case but due to larger side channels, a segment of droplets escaped from there hence rendering this unsuitable.

In Figure 2.14 a, the width is 335 μm and the width of pillar is increased by 10 μm for first four pillars and then it increases by 5 μm. In this case two consecutive droplets merged which was the requirement. Moreover no side flow

was observed thereby making it the optimized geometry.
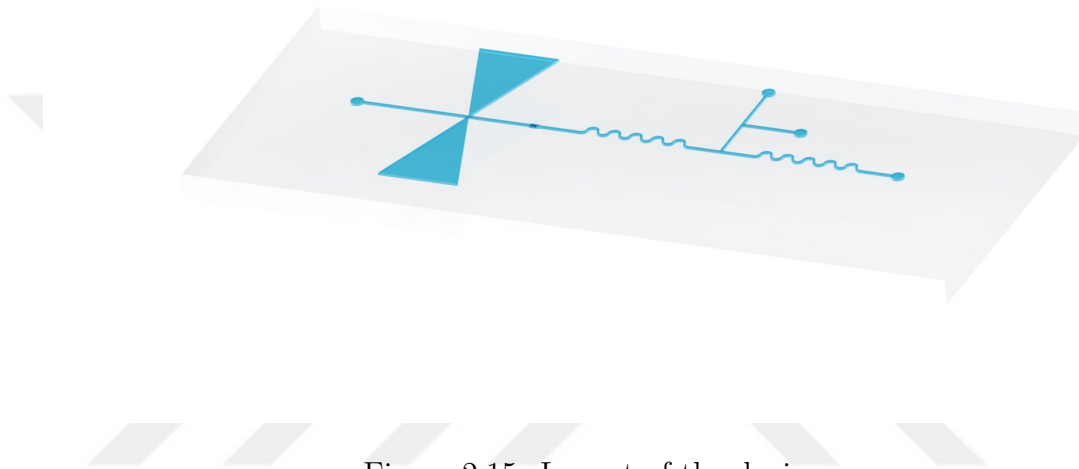
Figure 2.15: Layout of the device

After some experiments another change was made in the design as shown in Figure 2.15. Another T junction was introduced downstream to generate ammonia droplets separately. And the fabricated device is shown in Figure 2.16.

Figure 2.16: Fabricated device

Chapter 3

Synthesis of Chitosan Coated Iron Oxide Nanoparticles

Chitosan coated nanoparticles have various applications ranging from drug delivery to being used as catalyst. Chitosan coated iron oxide nanoparticles have been synthesized using batch wise synthesis technique. He et al. [75] synthesized Chitosan coated nanoparticles by mixing chitosan solution with iron chloride solution and then adding ammonia solution drop wise to initiate reaction.

3.1 Batch-wise Synthesis of Chitosan Coated Iron Oxide Nanoparticles

In order to optimize the recipe for microfluidic synthesis of chitosan coated iron-oxide nanoparticles batch wise synthesis was performed. Recipe reported by He et al. [75] was used.

Experiment 3.1 :

0.75g of Chitosan was dissolved in 100 mL of 0.3% acetic acid by continuous

stirring for 30 minutes. 1.09g of Fe(III) chloride and 0.4g of Fe(II) chloride was dissolved in 100 mL of water. Then both solutions were mixed by magnetic stirrer for two hours at room temperature. Finally 100mL of 28% ammonia solution was added drop wise and mixture was stirred for another two hours at 95°C. After that nanoparticles were centrifuged and solvents were removed and diluted in water.

Table 3.1: Chitosan coated iron oxide nanoparticle synthesis: Batch-wise reaction: Experiment 3.1

Batch synthesis	
Reaction Time	6 hours
Average Size	7.4 ±1.5 nm
Number of Measured Particles	40

(a)

(b)

(c)

(d)
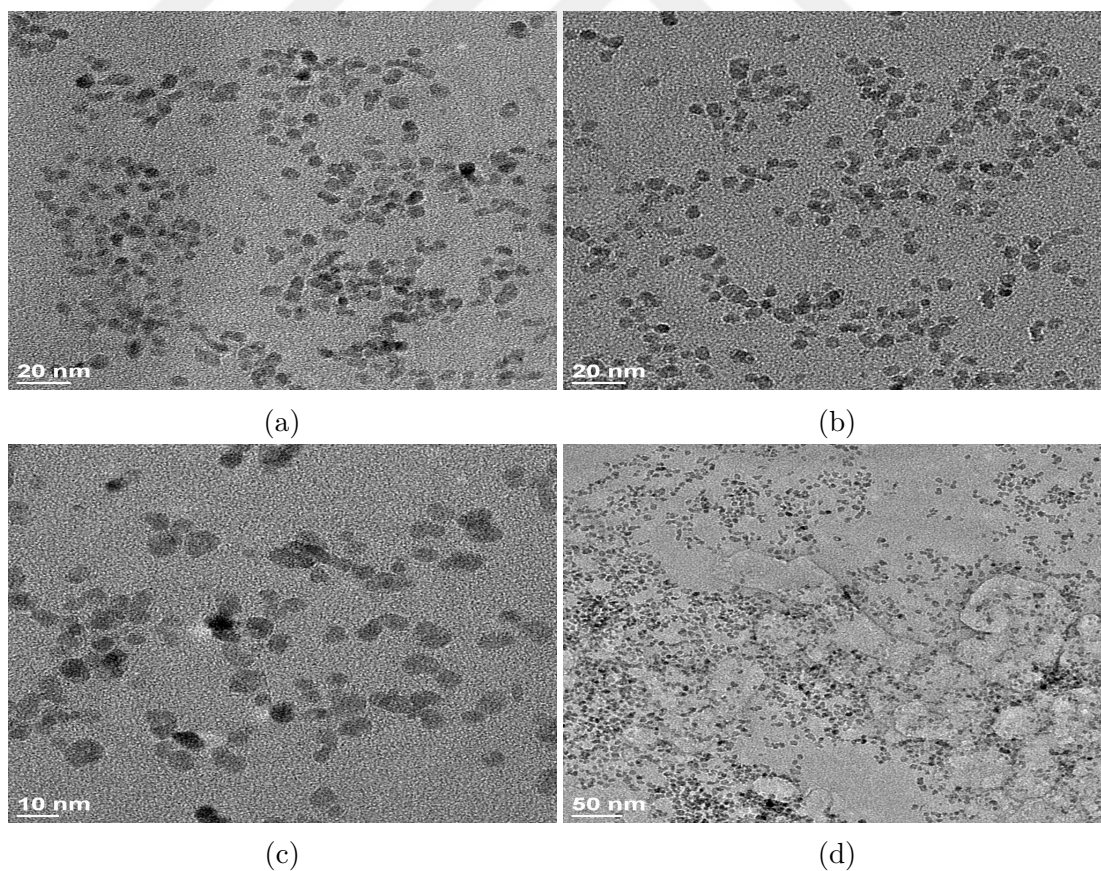
Figure 3.1: TEM images for batch-wise synthesis (Experiment 3.1)

Another synthesis (Experiment 3.2) was performed with lower concentration

of ammonia. Instead of 28%, it was diluted to 14% to see the effect of ammonia concentration. This was done to see if concentration changes anything in the final product as in microfluidic reactor it would be desirable to use less concentration of ammonia. Everything else was kept same as in Experiment 3.1.

Table 3.2: Chitosan coated iron oxide nanoparticle synthesis: Batch-wise reaction: Experiment 3.2

Batch synthesis	
Reaction Time	6 hours
Average Size	7.4 ±1.4 nm
Number of Measured Particles	40

(a)

(b)

(c)

(d)
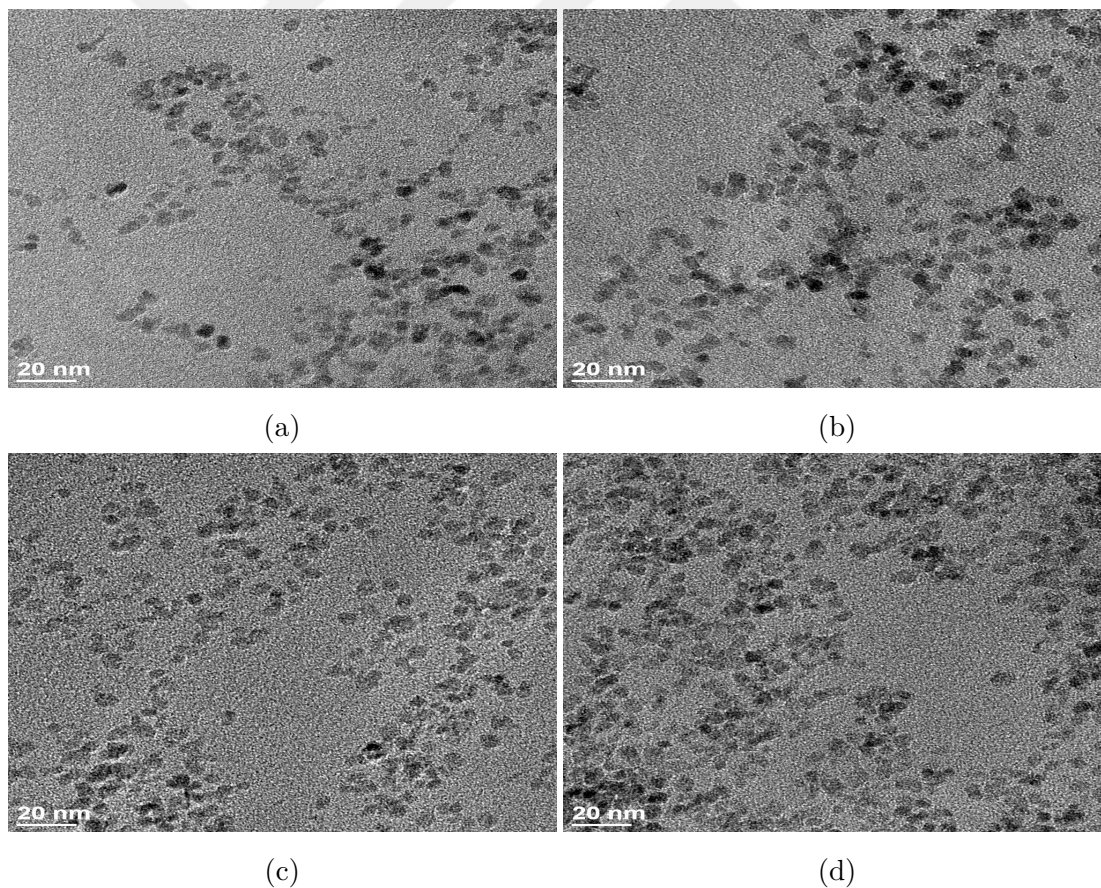
Figure 3.2: TEM images for batch-wise synthesis (Experiment 3.2)

Decreasing the concentration of ammonia did not have a major effect on the nanoparticles size. The residence time was also similar in both the cases. As

Table 3.3: EDX data

Element	Percentage
Fe	33.13
O	66.86

ammonia is being used to change pH so that the reaction can start, hence reducing the concentration to half did not have significant effect.

3.2 Synthesis of Chitosan Coated Iron oxide Nanoparticles Using Microreactor

Design of the microreactor has been described in detail in Chapter 2. After designing and fabrication of each microreactor, DI water and silicon oil were used to identify and optimize flow configuration. Then those flow configurations were used with chemical reagents to synthesize nanoparticles. Device layout is shown in Figure 3.3.
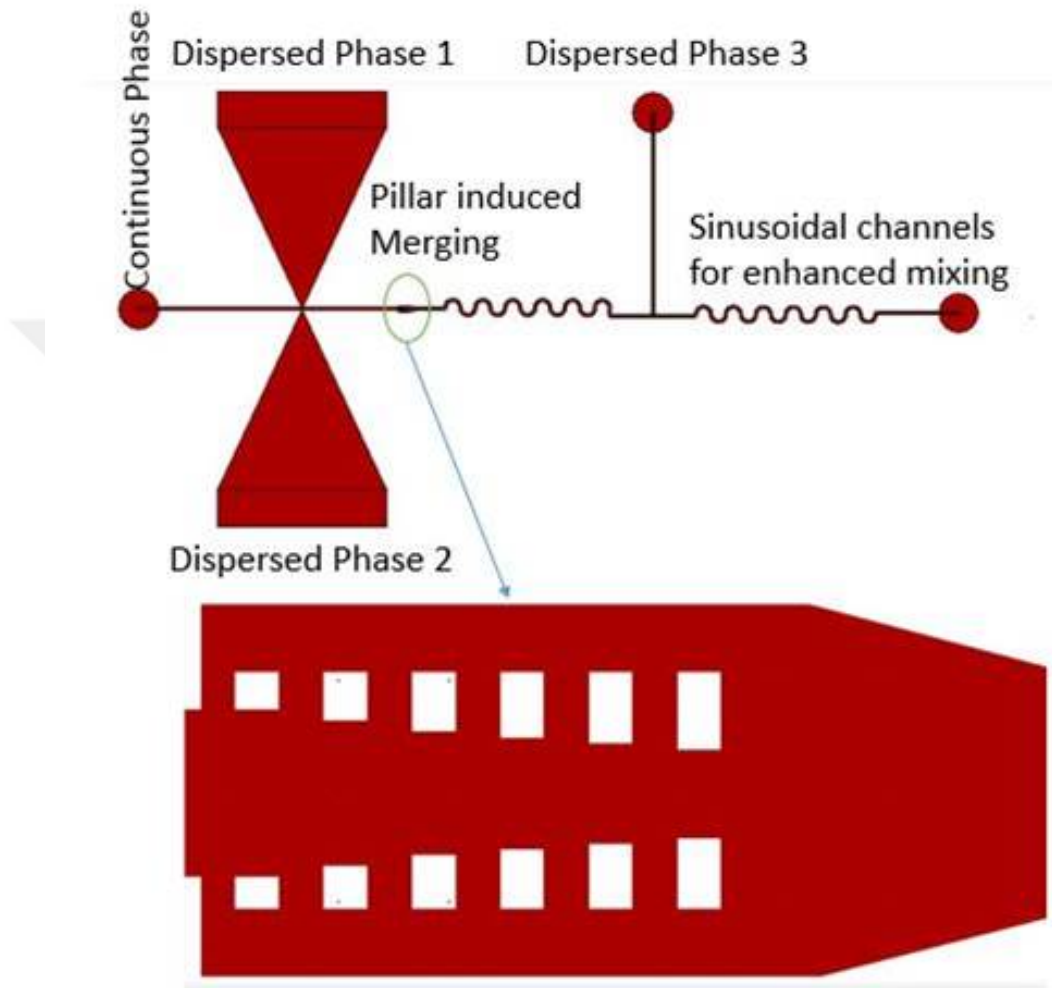
Figure 3.3: Layout of the device

The dimensions of main channels were 150 μm $\times$100 μm. Double T junction tapered inlets were used for alternating droplet generation and pillar structure was used for merging two consecutive droplets. Serpentine channels enhanced mixing by stretching and folding within a droplet.

3.2.1 Materials

For the synthesis of chitosan coated iron oxide nanoparticles in microfluidic reactor the recipe reported by He et al. was used [75]. Chemicals were ordered from SigmaAldrich, solutions were prepared in DI water obtained. 0.75g of chitosan was dissolved in 100 mL of 0.3% acetic acid by continuous stirring for 30 minutes. 1.09g of Fe(III) chloride and 0.4g of Fe(II) chloride was dissolved in 100 mL of water. These two solutions were used as dispersed phase 1 and 2 as shown in Figure 3.3 at tapered inlets. Initially olive oil was used as the continuous phase which was later replaced by silicon oil. Ammonia solution was used as dispersed phase 3.

3.2.2 Experimental Set-up

Experiments were performed at the microfluidics laboratory located in the Mechanical Engineering Department. Experimental set-up is shown in Figure 3.4

As shown in Figure 3.4 all the reagents were supplied using syringe pumps. Capillary tubing were used to transport fluids from syringes to inlets. An inverted microscope was used to observe the process going on in the channels. It can be viewed and recorded using camera and computer as shown in Figure 3.4. Flow rates can be easily controlled by using syringe pumps.
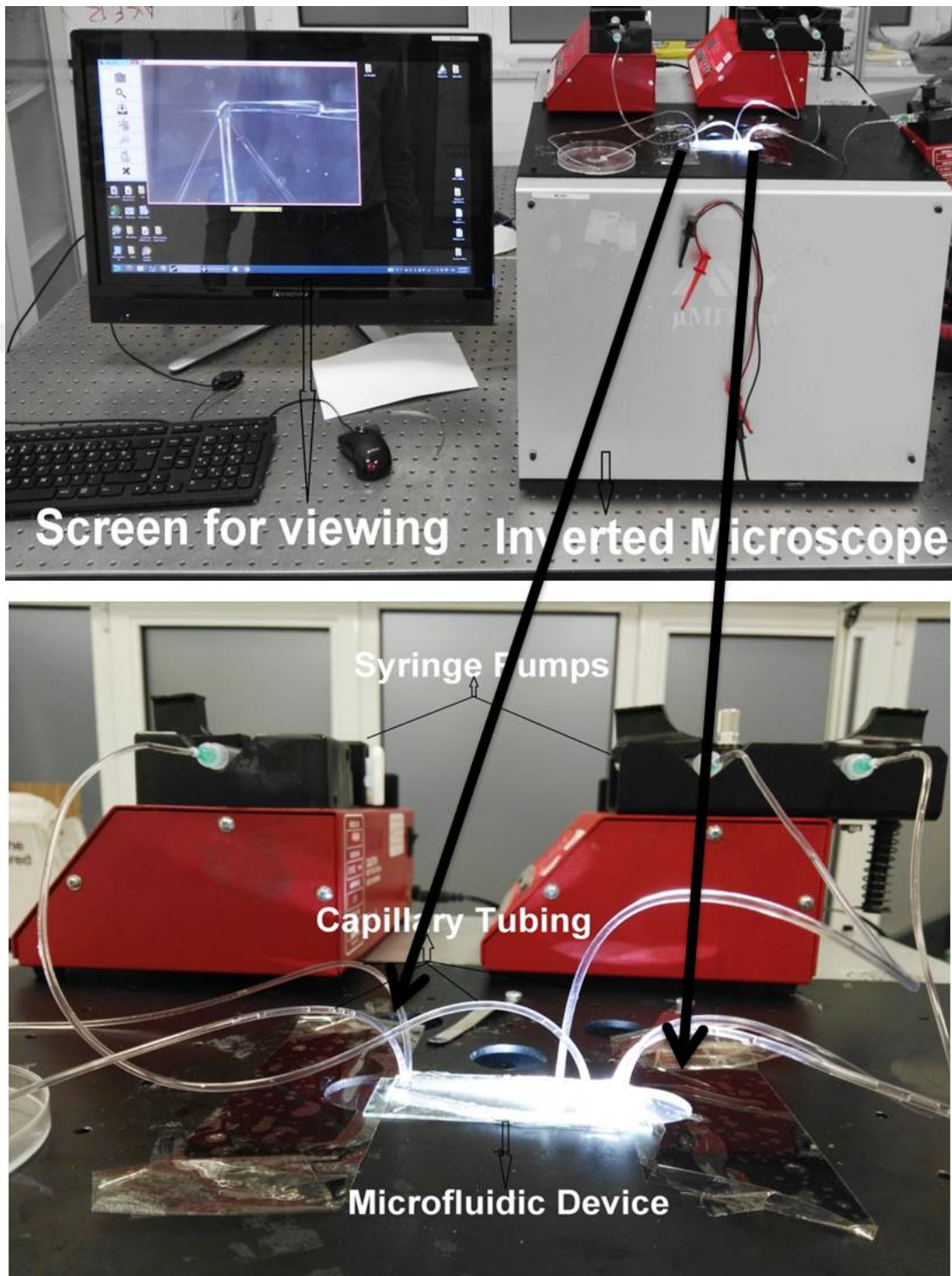
Figure 3.4: Experimental set-up: Solutions are pumped by the syringe pumps through the capillary tubing. A constant monitoring of the channels is available through the microscope.

3.2.3 Experiments

After preparing devices and connecting capillary tubing for inlets, oil was introduced in the channels until whole device was filled with oil. During the plasma bonding process, surface is modified and it became hydrophilic. In order to make the surface hydrophobic again, it's necessary to wet the channels with oil. This makes the surface hydrophobic again and facilitates the formation of droplets. After filling the whole device with oil, reagents are supplied and the process is observed using an optical microscope.

3.2.3.1 Alternating droplet generation

In order for the reaction to take place chitosan and iron chloride solutions need to mixed in 1:1, which implies that the size of the droplets should be identical. As described by Saqib et al. [76] tapered angle of 25°at inlets gives the highest efficiency of repetition of a pattern with uniform size and spacing of droplets. Figure 3.5 shows a sequence of droplet generation. Droplets are generated from both iron chloride solution and chitosan solution alternatively.
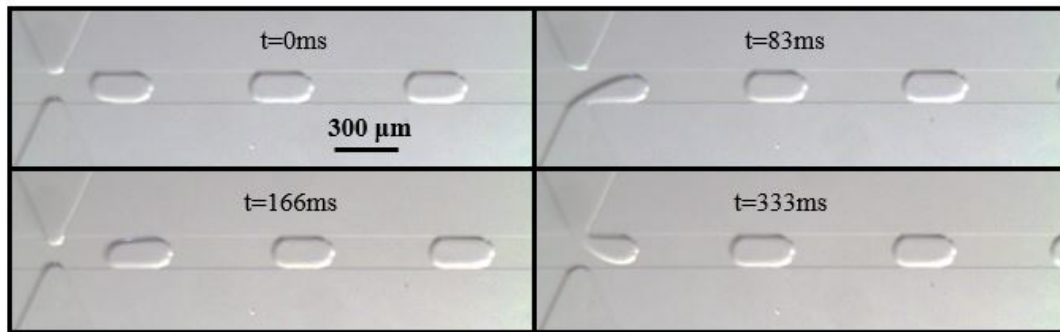
Figure 3.5: Alternating droplet generation using tapered inlets. Tapered geometry controls the pressure at the junction which enables the formation of droplets in a sequence.

As shown in Figure 3.5 first the lower stream enter the main channel and generates a droplet. After droplet generation the pressure at that side of the

junction reduces and the upper stream pushes the lower stream back into side channel. This causes the upper stream to enter the main channel and a droplet from that stream is generated. This process continues and droplets of each reagent are formed alternatively.

3.2.3.2 Droplet merging

After droplet generation, one droplet of each reagent have to be merged. In order for two droplets to merge pillar induced geometry is introduced. The width of channel is extended from 150 μm to 335 μm which slows down the droplets to such extent that only two consecutive droplets are merged. Figure 3.6 shows two consecutive iron chloride and chitosan solution droplets merging in the pillar structure.
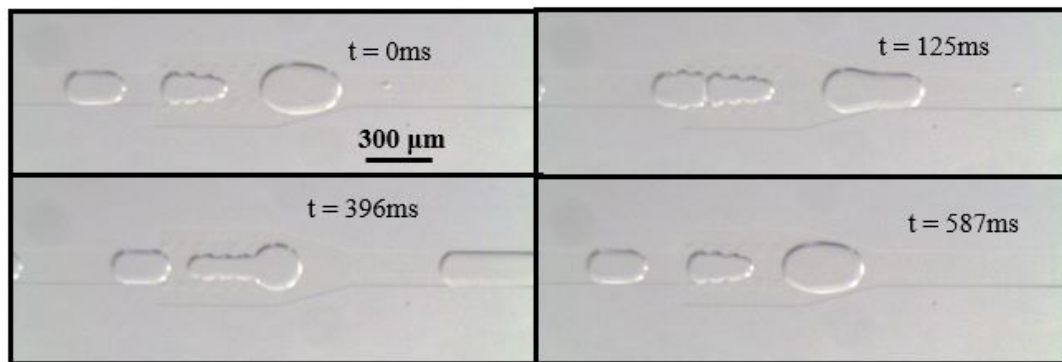
Figure 3.6: Passive merging of alternating droplets in pillar induced structure.

As shown in Figure 3.6 first a droplet reaches the extended channel and almost comes to rest in pillars. Then consecutive droplet enters the channel and contacts with the droplet that is already there. These two droplets merge and then are pushed out of the pillars to enter the main channel again.

3.2.3.3 Addition of Ammonia

After merging, the resulting droplet passes through the serpentine channel where mixing of two reagents takes place. After mixing ammonia solution is added to start the reaction. Ammonia solution has been added in two ways in the experiments.

In the first method, the device shown in Figure 2.12 was used. Ammonia was added as the third dispersed phase and while entering main channel, it formed a droplet and merged with droplet containing chitosan and iron chloride.
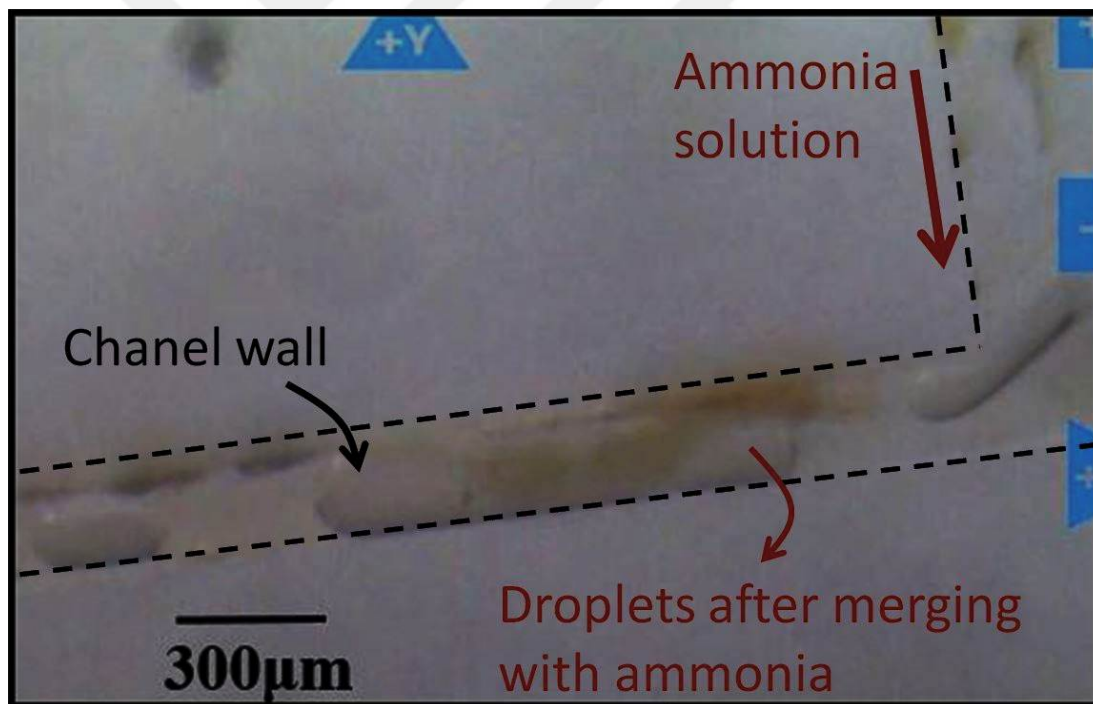
Figure 3.7: Merging of ammonia to initiate reaction

Figure 3.7 shows the merging of ammonia, the yellow colour signifies the oxidation of iron and is a proof of reaction taking place in droplet. But the device shown in Figure 2.12 was not promising when it comes to merging of ammonia there were minor in consistencies.

In order to address that issue, another T junction was introduced downstream

to facilitate ammonia droplet formation as shown in Figure 2.15. In this device ammonia forms a droplet at the T junction and then that droplet enters the main channel and merge with droplet to start reaction. The sequence of merging is shown in Figures 3.8 , 3.9 , 3.10 and 3.11.
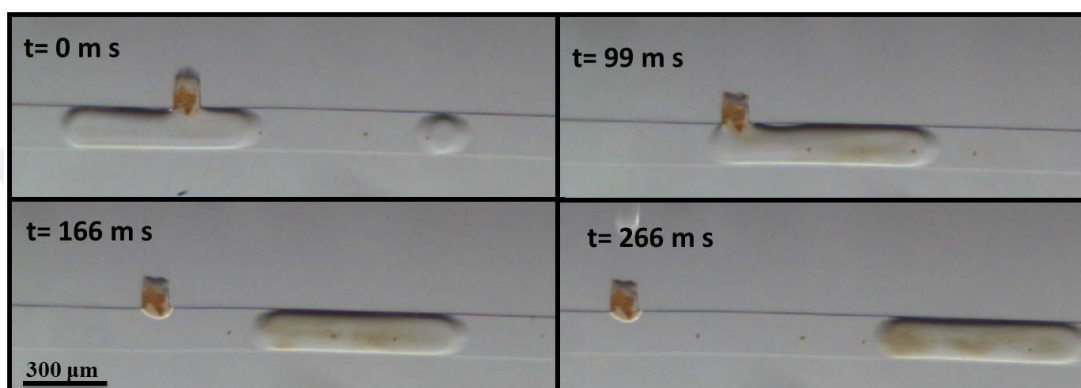
Figure 3.8: Merging of ammonia droplet to initiate reaction
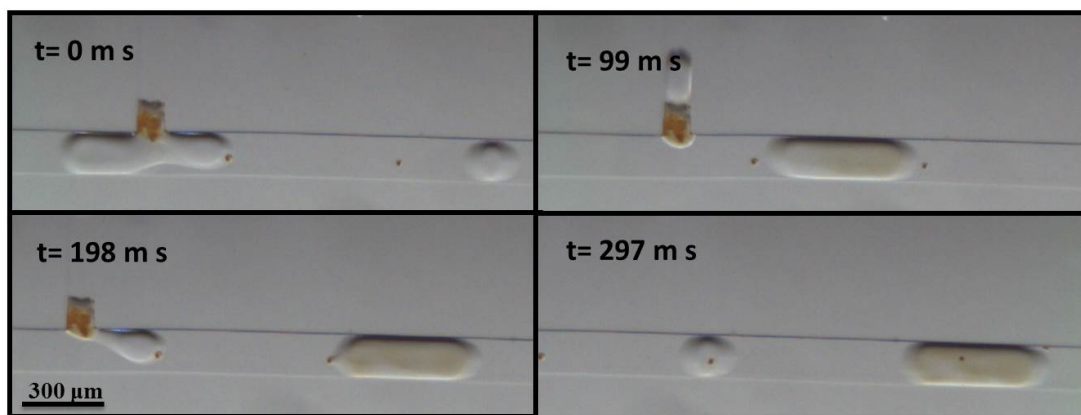
Figure 3.9: Merging of ammonia droplet to initiate reaction

As shown in Figures 3.8 , 3.9 , 3.10 and 3.11 ammonia droplet enters the main channel and comes in contact with already merged droplet of chitosan and iron chloride. Both droplets merge and reaction starts. Yellowish colour is due to the oxidation of iron to iron oxide and it shows the start of reaction. Then mixing takes place in serpentine channels and nanoparticles are collected at the outlet.
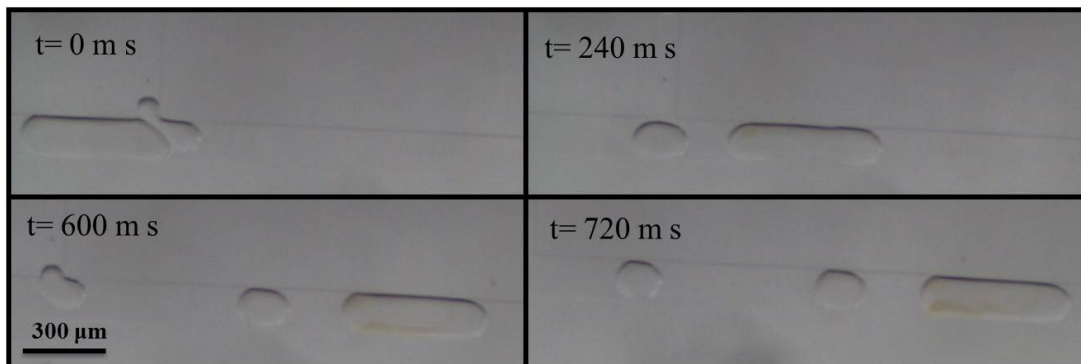
Figure 3.10: Merging of ammonia droplet to initiate reaction
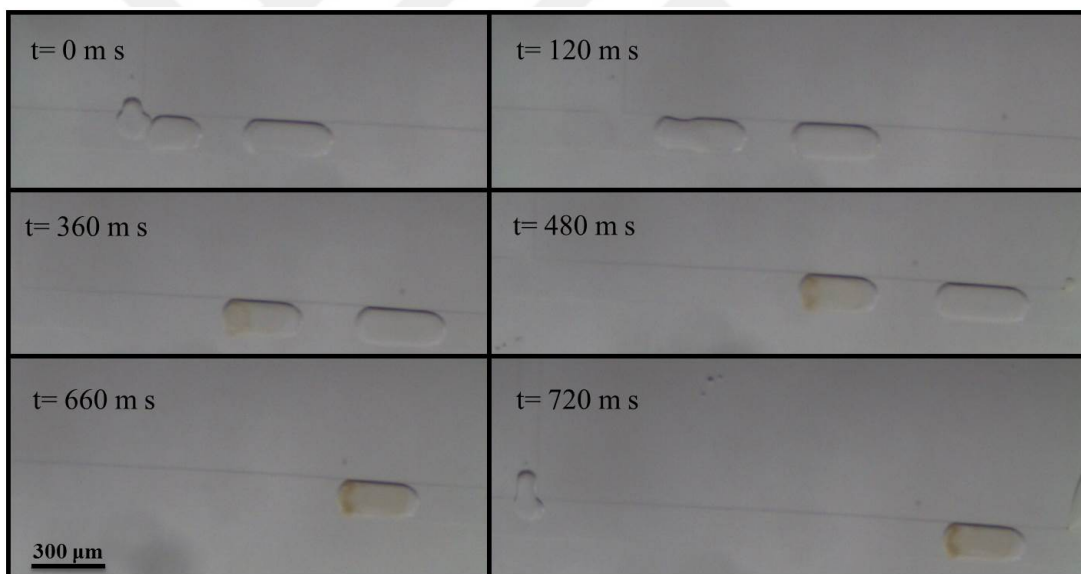
Figure 3.11: Merging of ammonia droplet to initiate reaction

3.2.4 Results

Collected nanoparticles were centrifuged to remove solvent and then were diluted in DI water. TEM analysis was done to observe the morphology and composition of nanoparticles. FTIR data was also plotted to confirm the presence of chitosan.

3.2.4.1 TEM Results:

Nanoparticles were observed under the TEM located at National Nanotechnology Research Center (UNAM).

Table 3.4: Chitosan coated iron oxide nanoparticle synthesis: Microreactor Synthesis: Experiment 3.3

Microreactor synthesis	
Average Size	8.5 ±1.3 nm
Number of Measured Particles	40

EDX data was also collected for the samples and is shown in Table 3.5. It clearly shows the presence of iron and oxygen in nanoparticles. As the grids are made of carbon and carbon is the dominant element in chitosan, EDX result can not prove the presence of chitosan conclusively. That is why FTIR spectra was also obtained.

Table 3.5: EDX data

Element	Percentage
Fe	44.19
O	55.8

(a)

(b)

(c)

(d)
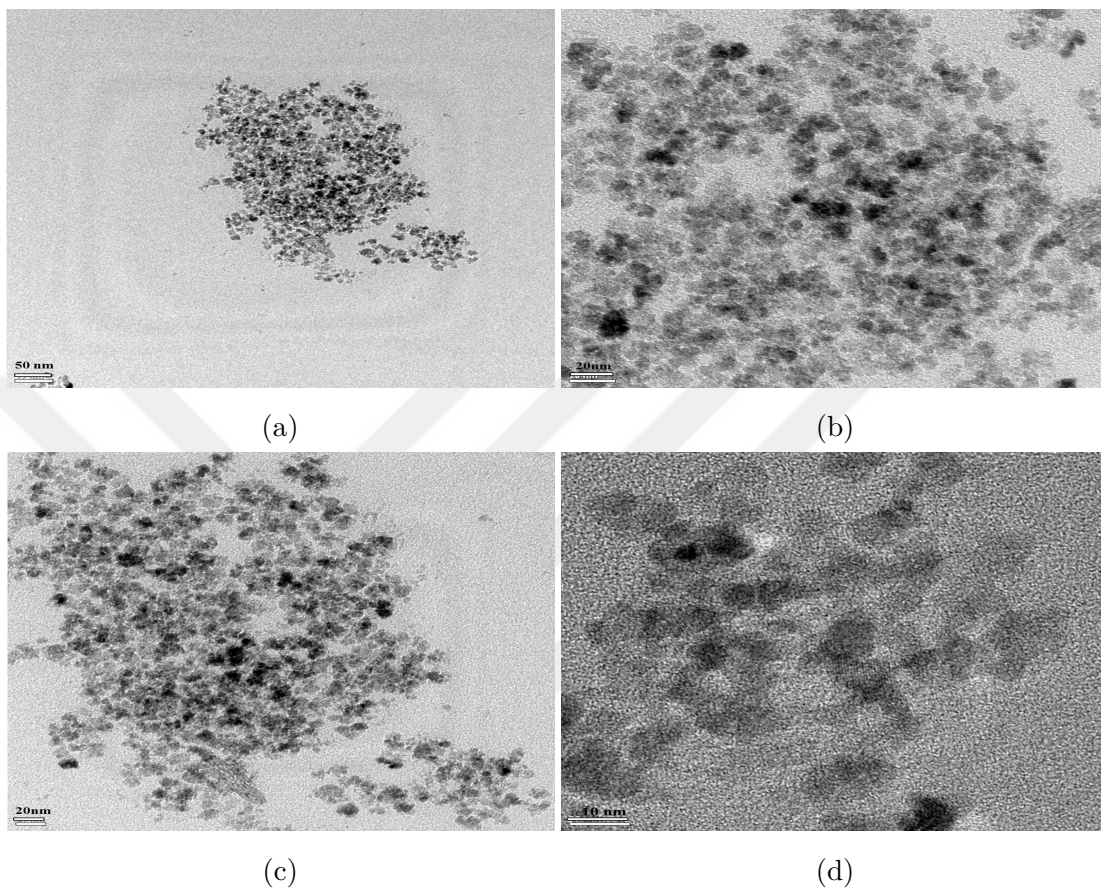
Figure 3.12: TEM images of nanoparticles obtained by microfluidic synthesis (Experiment 3.3)

3.2.4.2 FTIR:

FTIR spectra was performed to confirm the presence of chitosan. FTIR data was plotted to compare the corresponding peaks and is presented in Figure 3.13.
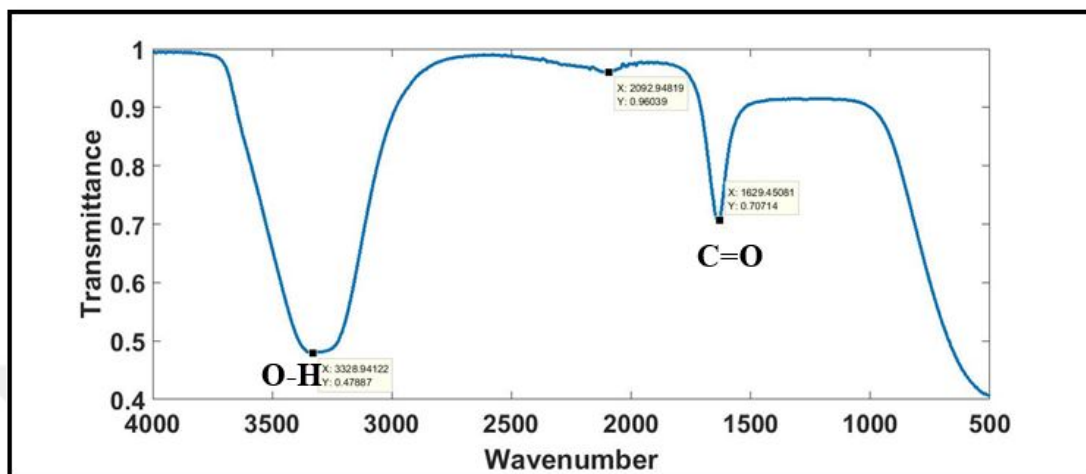
Figure 3.13: FTIR spectra of nanoparticles

Chitosan presence in the nanoparticles is identified using the FTIR analysis. Successful coating of iron-oxide nanoparticles with chitosan is confirmed by the appearance of characteristic bands like OH at 3330 cm^{-1} and C=O at 1629 cm^{-1} [72]. TEM results together with FTIR demonstrate the synthesis of chitosan coated iron-oxide nanoparticles.

3.2.5 Conclusion

Following table provide a comparison between batch wise synthesis and microfluidic synthesis.

Table 3.6: Comparison of size of nanoparticles

Synthesis technique	Average size	Coefficient of variation
Microfluidic	8.5 ±1.3 nm	0.15
Batch 1	7.4 ±1.5 nm	0.20
batch 2	7.4 ±1.4 nm	0.18

Table 3.6 shows a comparison between size of nanoparticles among two batch wise techniques and microfluidic synthesis. It can be seen that coefficient of variation is small ac compared to batch wise techniques.

Synthesis of chitosan coated iron-oxide nanoparticles have been realized for the first time using a microfluidic platform which resulted in a narrower size distribution compared to the batch-wise methods. Residence time has been significantly reduced as compared to batch-wise synthesis. Alternating droplet formation , merging and mixing was realized in single chip. Dimensions of device were optimized and flow rate of reagents were adjusted that resulted in autonomous process from formation of droplet to the precipitation. There were a few issues like merging of ammonia droplet was not consistent all the time. Changing the continuous phase from olive oil to silicon helped in stable droplet generation from ammonia. Silicon oil was very compatible when it came to formation of ammonia droplets. However chitosan droplets formation was effected by this change, which was tackled by varying the viscosity of silicon oil. Further research can be carried out to find a better continuous phase which is both inert and has acceptable range of viscosity and surface tension to form droplets from all three regents and merge.

Chapter 4

Synthesis of Hydroxyapatite in the Microreactor

Hydroxyapatite ($\text{Ca}_5(PO_4)_3OH$ hereafter HA) is a naturally occurring calcium phosphate and is the mineral component of human hard tissues [78]. Therefore nanohydroxyapatite (nano-HA) has been of interest as a biomaterial for orthopedic applications. Its outstanding properties like biocompatibility, bioactivity and osteoconductivity makes it very suitable for various applications ranging from bone tissue engineering to mineralizing agent in toothpastes to drug and gene delivery [79].

69% of the bone tissue is composed of HA which provides stiffness to bone structure and makes HA an important ceramic in orthopedic applications. Nano-HA has quicker response in implant surface turnover in implants in marrow cavity [80]. Muller-Mai et al. showed that nano-HA can be used for bone implants and drug release [81]. HA can be also used as a component in composite systems such as HA-chitosan-collagen [82] and collagen [83, 84, 85] for tissue engineering where HA provides stiffness and osteoconduction. Nano-HA can also be used in drug delivery systems [86, 87].

4.1 Synthesis of Hydroxyapatite

Hydroxyapatite $(Ca_5(PO_4)_3OH)$ is synthesized using various techniques, some of which are:

1) Wet chemical synthesis

2) Dry chemical synthesis

3) Vapour phase reaction

Each of these methods has its own advantages and drawbacks. In case of wet chemical synthesis, water is the main by-product which is not harmful and can be easily removed from the system. Although this technique is practical and cost-effective, its very sensitive to reaction conditions. In case of dry chemical process, the reactions are easily reproducible but there is high risk of contamination [88, 89, 90].

Wet chemical synthesis is usually performed using precipitation, hydrothermal, hydrolysis and sol-gel techniques out of which precipitation is very common. Precipitation reactions are inexpensive and produce high purity HA samples [90]. Since it is an important issue to obtain nano-HA particles with spherical shape and homogenous particle sizes, the microfluidic devices designed as part of this work was also used for the precipitation reaction.

4.1.1 Materials

Chemical precipitation uses inorganic oxide solution to form HA [91]. In this case calcium nitrate $(Ca(NO_3)_2 \cdot 4\,H_2O)$ and diammonium phosphate $((NH_4)_2HPO_4)$ were used as the starting materials.

4.1.2 Microfluidic Device

PDMS based microfluidic device was used with one T junction. Fabrication procedure is same as described in Section 2.1. Figure 4.1 shows the T-junction for droplet generation using olive oil as the continuous phase.
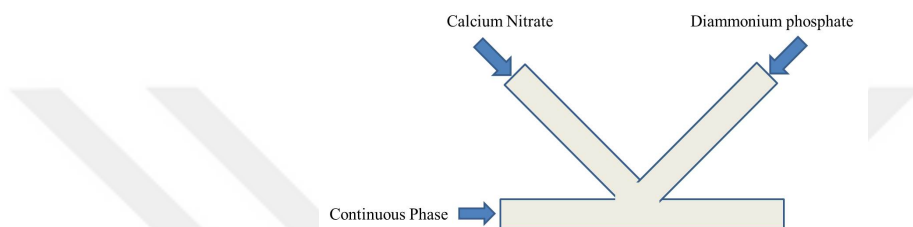
Figure 4.1: Synthesis of Hydroxyapatite using droplet based microreactor

Aqueous solutions of calcium nitrate and diammonium phosphate are used as dispersed phases and olive oil has been used as the continuous phase. Reagents make contact with each other at the junction and create an emulsion in oil. Emulsions are then transported to the outlet where nanoparticles are collected.

4.1.3 Experiments

Experimental set-up shown in 3.4 was used for this synthesis as well. Both the reagents and olive oil were introduced using syringe pumps and the droplet formation was observed using a microscope and a CCD camera. As shown in Figure 4.2 both reagents come in contact at the T-junction and form a single droplet.
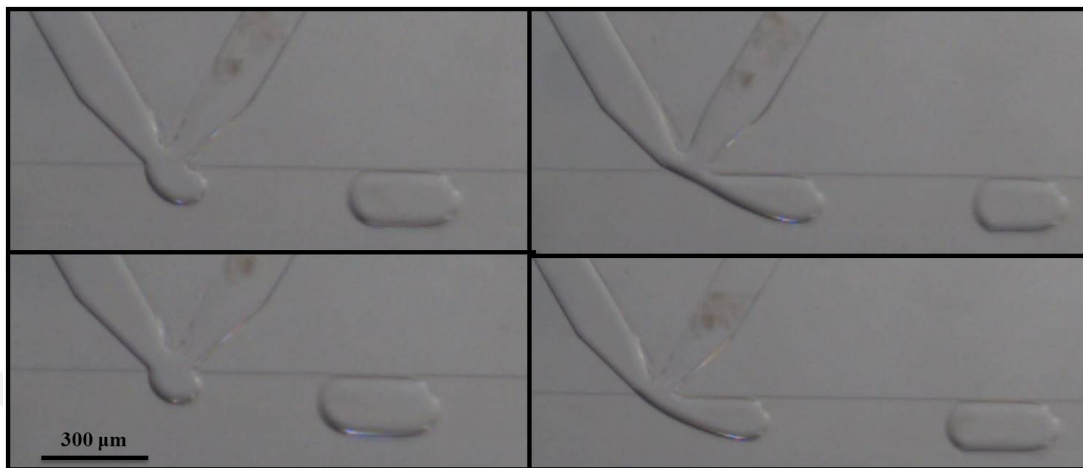
Figure 4.2: Snapshot of droplet generation taken during experiment

Precipitation reaction takes place as reagents mix within the droplets, finally nanoparticles are collected at the outlet. Experiments were performed with varying concentration of reactants.

4.1.4 Results

HA particles were observed under the SEM to find out the particle shape and size of the obtained nanoparticles.. Results from experiments with varying concentration are presented below.

Experiment 4.1:

In this experiment 0.5 M calcium nitrate $(Ca(NO_3)_2 \cdot 4\,H_2O)$ and 0.3 M di-ammonium phosphate $((NH_4)_2HPO_4)$ solution were used. Concentrations of the solutions were arranged considering the (Ca/P) molar ratio which is 1.67 for synthetic HA. Figure 4.3 shows the SEM micro-graphs for the synthesis.
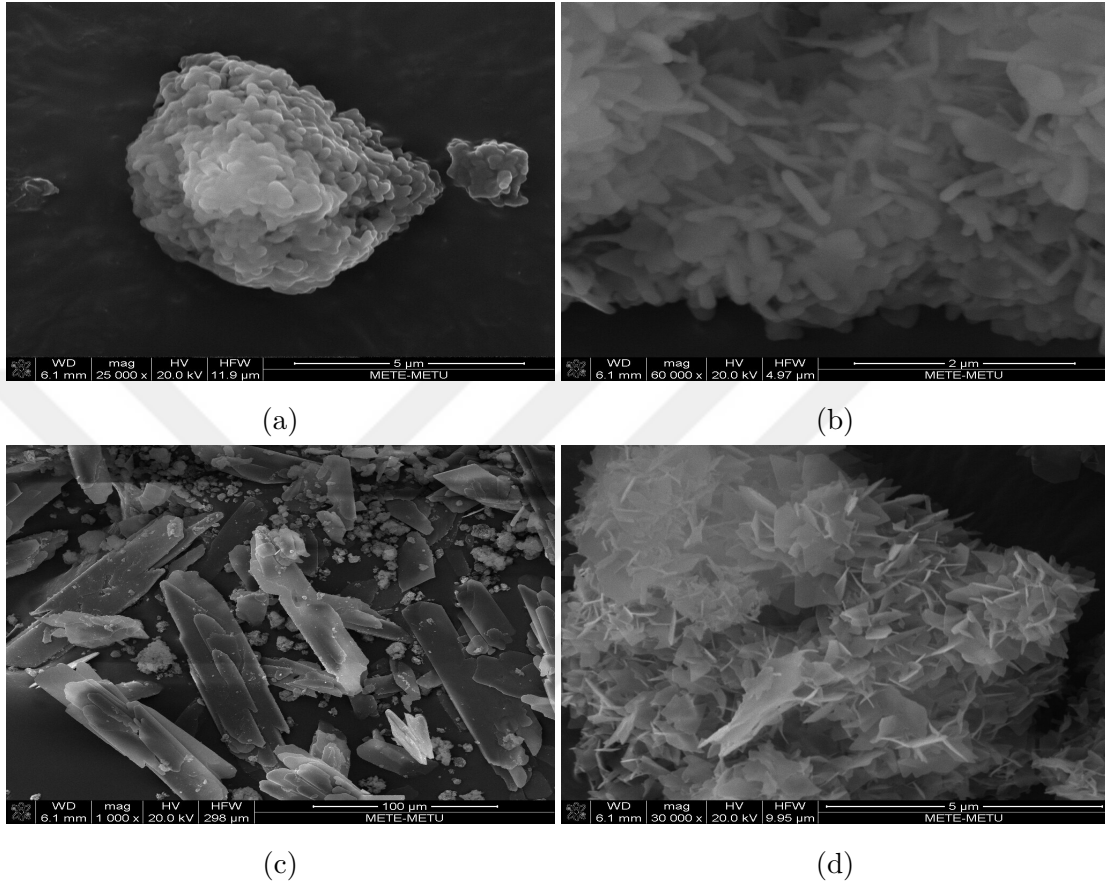
Figure 4.3: SEM images of Hydroxyapatite (Experiment 4.1)

Reaction rate for the reactants for quite high so the reaction was taking place the immediately after the reagents come in contact with each other. Due to high reaction rate the precipitates were clogging the main channel which results in high back pressure thereby hindering the flow. Also spherical monodisperse nanoparticles were expected but SEM images shows varying size as well as the agglomeration of nanoparticles.

Experiment 4.2:

In order to reduce the rate of reaction and increase the residence time so that the reagents should react closer to outlet, the concentration of both the solutions were lowered but concentrations of the solutions were arranged considering the (Ca/P) molar ratio which is 1.67 for synthetic HA. In this experiment the

concentration of calcium nitrate was decreased to 0.25 M and concentration of diammonium phosphate to 0.15 M, which is half the concentration used in experiment 4.1. Figure 4.4 shows SEM images for synthesis.

<div align="center">(a)   (b)</div>
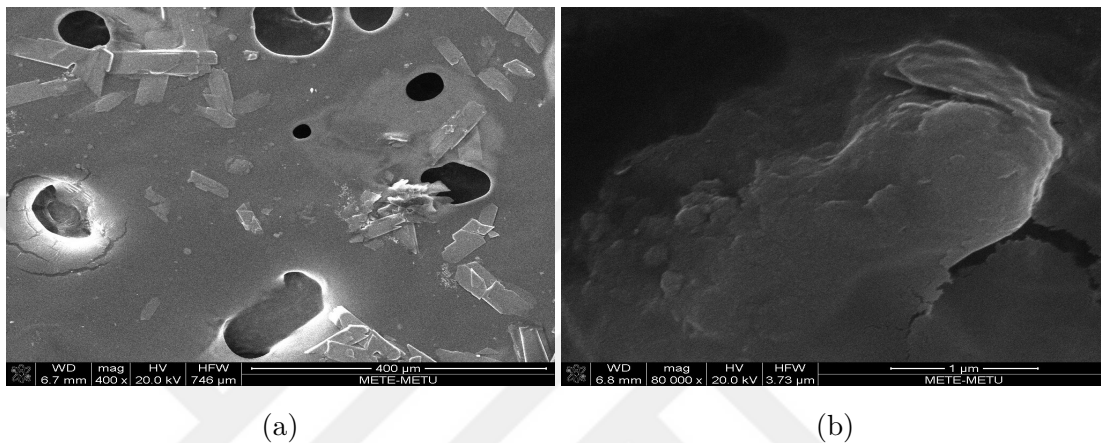
Figure 4.4: SEM images of Hydroxyapatite (Experiment 4.2)

Reduced concentration decreased the reaction rate, however channels were still getting clogged. And the yield of reaction was decreased. Agglomeration was still an issue and the particle size and morphology was not up to expectations. As shown in SEM images particles are not spherical and vary in size.

Experiment 4.3:

This experiment was performed with much lower concentration than experiment 4.2. 0.125 M calcium nitrate $(Ca(NO_3)_2 \cdot 4\,H_2O)$ and 0.075 M diammonium phosphate $((NH_4)_2HPO_4)$ were prepared (4 times less than the experiment 4.1). Reducing the concentration to this extent eliminated a few problems related to the clogging of the channels. Residence time increased and slow reaction prevented clogging of channels for long time. It was easier to transport the nanoparticles by the continuous phase. Figure 4.5 shows the SEM images.

(a)   (b)

(c)   (d)

(e)   (f)
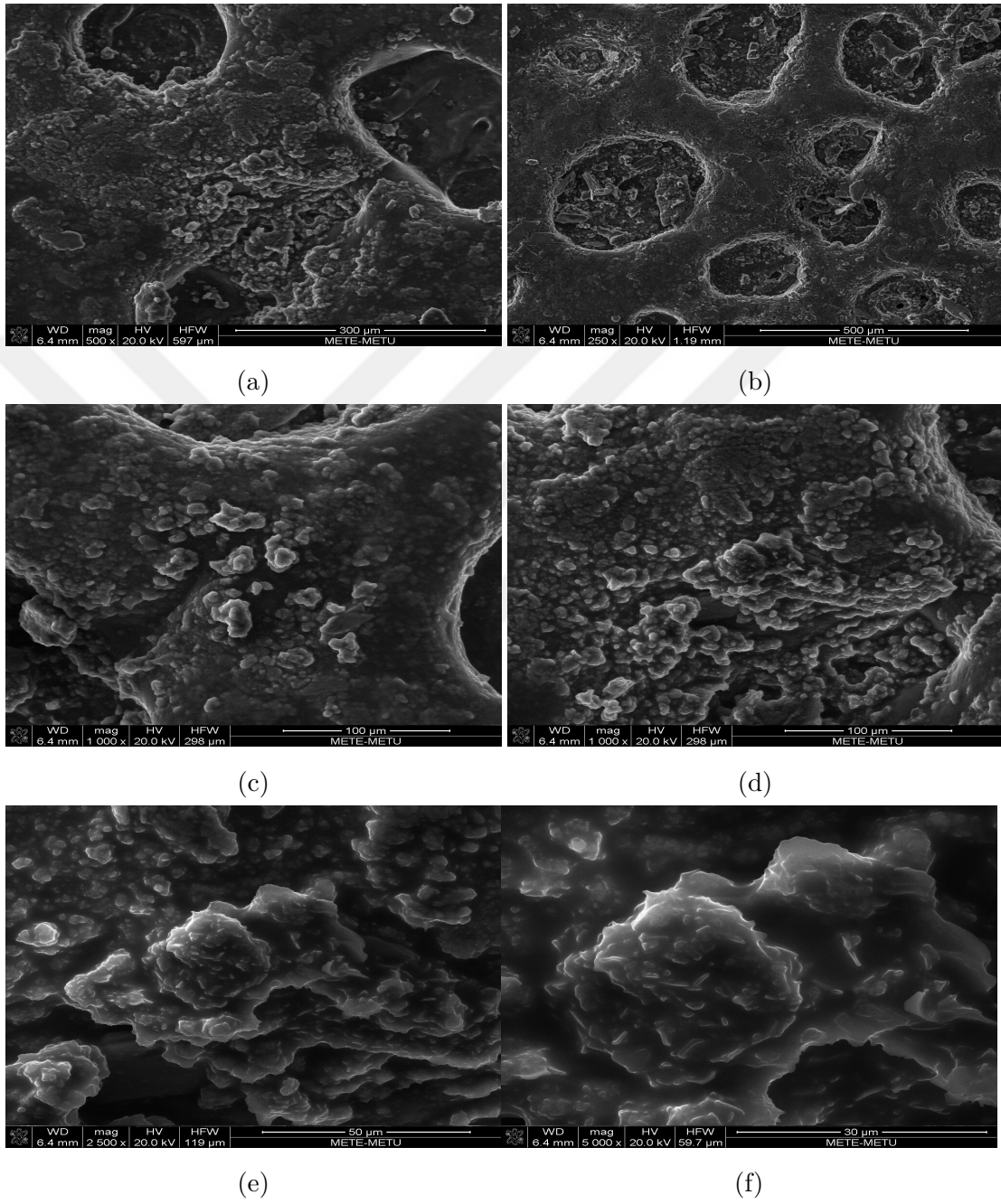
Figure 4.5: SEM images of Hydroxyapatite synthesized with lower concentration (Experiment 4.3)

Decreased concentration increased the residence time and clogging problem was solved to an extent. However after some time the clogging took place thereby

stopping the process. Nanoparticles had some agglomeration however the shape of nanoparticles were quite consistent. As the particles are not perfectly spherical but it can be seen that there is consistency in shape. However microfluidics devices was aimed to produce spherical nanoparticles with uniform size.

4.1.5 Conclusion

Synthesis of nano hydroxyapatite was realized in microfluidic device using various concentration of precursors solution. The concentration was varied and adjusted to keep constant the (Ca/P) molar ratio which is 1.67 for synthetic HA. Higher concentration of solutions resulted in clogging of channels and thereby disrupting the flow. But as the concentration was reduced the clogging was reduced but not eliminated. Shape of nanoparticles were improved with decreasing concentration however agglomeration was still a major issue. Further experiments could be performed at even lower concentration to facilitate the continuous synthesis with uniform size and shape.

Chapter 5

Conclusion and Recommendations for Future Work

In this thesis, a microfluidic reactor was designed and fabricated by soft-lithography. Microreactor consists of three essential components integrated in a single chip: alternating droplet formation zone, a merging zone and a mixing zone. Microreactor had precise control over reaction conditions such as mixing, reagent concentration and residence time. Optimum flow conditions were investigated first by using only water. Later on chitosan coated iron oxide nanoparticles were synthesized at those optimum flow conditions. The result of synthesis was quite promising and it showed narrower size distribution as compared to the batch-wise synthesis. Residence time for batch-wise synthesis was 6 hours but it takes seconds for reaction to take place in the microreactor. Moreover the amount of reagents required was quite low. Hence all these advantages make microfluidic synthesis preferable over batch-wise synthesis.

The encapsulation of iron oxide nanoparticles in chitosan has been successfully achieved with size of 8.5 $\pm$1.3 nm, however further investigation on the synthesis of super-magnetic iron oxide is required. For instance one of the problems in

microfluidic reactor was in the merging of ammonia droplet with other reagents. The droplet merging has not been successful at all times. Hence some further improvements are required to make it consistent. Mixing in the droplets was quite successful, however sometimes precipitates stick to the channel walls causing clogging. Though it was not major problems as continuous flow usually could get rid of the clogging in no time, just slowing down the process. Therefore using solutions with lower concentrations might circumnavigate this issue. Also a pathway to encapsulate drug in nanoparticles is needed to be investigated as well as in-vivo or in-vitro experiments on drug release will help understand the efficiency of drug loading and release.

In addition to chitosan coated nanoparticles synthesis, synthesis experiments were also conducted for hydroxyapatite nanoparticle synthesis. HA is a well-known bioactive ceramic material that is used in various biomedical applications such as orthopedic, ophthalmology and dentistry. HA is the inorganic constituent of the hard tissues and can be prepared in different morphologies like granules, powders, coatings, porous blocks, etc. However, production of nano-sized HA particles have gained significant attention recently. Since conventional synthesis techniques display difficulties with obtaining particles with a distinct shape and homogeneous particle size distribution, microfluidics approach may be a promising solution for this issue. Microfluidics enables to achieve spherical shaped nanoparticles with a certain particle size due to the usage of 2 same diameter channels where the precursor solutions flow. Hence, diversity in the shape and size of the nanoparticles will be reduced and the effect of the particle size and shape on the properties of the nanoparticles will be eliminated. However, troubles were faced during the experiments carried out to synthesize HA nanoparticles. Clogging was the main obstacle that stops the progress of the process. As the HA nanoparticles immediately precipitate when Ca and P solution drops react with each other and the product get stuck in the channels. Although the concentration of the Ca and P source solutions were pretty diluted and different microfluidics devices were tested, the results were not sufficient enough. Because the particle shape and size properties were not in the way that was expected. Therefore, further experiments should be realized with much more diluted solutions and/or

different starting precursors to have HA nanoparticles with reliable properties.

Bibliography

[1] N. Bremond, A. R. Thiam, and J. Bibette, "Decompressing emulsion droplets favors coalescence," *Physical review letters*, vol. 100, no. 2, p. 024501, 2008.

[2] K. N. M. Y. T. Hosokawa, M.; Nogi, "Nanotechnology handbook," 2007.

[3] C. Mah, T. J. Fraites, I. Zolotukhin, S. Song, T. R. Flotte, J. Dobson, C. Batich, and B. J. Byrne, "Improved method of recombinant aav2 delivery for systemic targeted gene therapy," *Molecular Therapy*, vol. 6, no. 1, pp. 106 – 112, 2002.

[4] H. J. B. F. K. E. B. J. M. S. P. M. B. A. Panatarotto D, Prtidos CD, "Immunization with peptide-functionalized carbon nanotubes enhances virus-specific neutralizing antibody responses," *ChemistryBiology*, vol. 10, no. 1, pp. 961 – 966, 2003.

[5] R. Mahtab, J. P. Rogers, and C. J. Murphy, "Protein-sized quantum dot luminescence can distinguish between "straight", "bent", and "kinked" oligonucleotides," *Journal of the American Chemical Society*, vol. 117, no. 35, pp. 9099–9100, 1995.

[6] J.-M. Nam, C. S. Thaxton, and C. A. Mirkin, "Nanoparticle-based bio-bar codes for the ultrasensitive detection of proteins," *Science*, vol. 301, no. 5641, pp. 1884–1886, 2003.

[7] M. D. Molday RS, "Immunospecific ferromagnetic iron-dextran reagents for the labeling and magnetic separation of cells.," *Journal of immunological methods*, vol. 52, no. 3, pp. 353–367, 1982.

[8] C.-H. Chang, B. Paul, V. Remcho, S. Atre, and J. E. Hutchison, "Synthesis and post-processing of nanomaterials using microreaction technology," *Journal of Nanoparticle Research*, vol. 10, pp. 965–980, 08 2008.

[9] E. Y. Erdem, J. C. Cheng, F. M. Doyle, and A. P. Pisano, "Multi-temperature zone, droplet-based microreactor for increased temperature control in nanoparticle synthesis," *Small*, vol. 10, no. 6, pp. 1076–1080, 2014.

[10] C.-X. Zhao, L. He, S. Z. Qiao, and A. P. Middelberg, "Nanoparticle synthesis in microreactors," *Chemical Engineering Science*, vol. 66, no. 7, pp. 1463–1479, 2011.

[11] L.-H. Hung and A. Lee, "Microfluidic devices for the synthesis of nanoparticles and biomaterials," *Journal of Medical and Biological Engineering*, vol. 27, pp. 1–6, 11 2006.

[12] T. Nisisako, S. Okushima, and T. Torii, "Controlled formulation of monodisperse double emulsions in a multiple-phase microfluidic system," *Soft Matter*, vol. 1, no. 1, pp. 23–27, 2005.

[13] S. Van der Graaf, M. Steegmans, R. Van Der Sman, C. Schroën, and R. Boom, "Droplet formation in a t-shaped microchannel junction: a model system for membrane emulsification," *Colloids and Surfaces A: Physicochemical and Engineering Aspects*, vol. 266, no. 1-3, pp. 106–116, 2005.

[14] P. Garstecki, M. J. Fuerstman, H. A. Stone, and G. M. Whitesides, "Formation of droplets and bubbles in a microfluidic t-junction—scaling and mechanism of break-up," *Lab on a Chip*, vol. 6, no. 3, pp. 437–446, 2006.

[15] J. Xu, S. Li, J. Tan, Y. Wang, and G. Luo, "Preparation of highly monodisperse droplet in a t-junction microfluidic device," *AIChE journal*, vol. 52, no. 9, pp. 3005–3010, 2006.

[16] Q. Xu and M. Nakajima, "The generation of highly monodisperse droplets through the breakup of hydrodynamically focused microthread in a microfluidic device," *Applied Physics Letters*, vol. 85, no. 17, pp. 3726–3728, 2004.

[17] L. Yobas, S. Martens, W.-L. Ong, and N. Ranganathan, "High-performance flow-focusing geometry for spontaneous generation of monodispersed droplets," *Lab on a Chip*, vol. 6, no. 8, pp. 1073–1079, 2006.

[18] B. D. Hamlington, B. Steinhaus, J. J. Feng, D. Link, M. J. Shelley, and A. Q. Shen, "Liquid crystal droplet production in a microfluidic device," *Liquid Crystals*, vol. 34, no. 7, pp. 861–870, 2007.

[19] I. Shestopalov, J. D. Tice, and R. F. Ismagilov, "Multi-step synthesis of nanoparticles performed on millisecond time scale in a microfluidic droplet-based system," *Lab on a Chip*, vol. 4, no. 4, pp. 316–321, 2004.

[20] L.-H. Hung, K. M. Choi, W.-Y. Tseng, Y.-C. Tan, K. J. Shea, and A. P. Lee, "Alternating droplet generation and controlled dynamic droplet fusion in microfluidic device for cds nanoparticle synthesis," *Lab on a Chip*, vol. 6, no. 2, pp. 174–178, 2006.

[21] E. M. Chan, A. P. Alivisatos, and R. A. Mathies, "High-temperature microfluidic synthesis of cdse nanocrystals in nanoliter droplets," *Journal of the American Chemical Society*, vol. 127, no. 40, pp. 13854–13861, 2005.

[22] B. K. Yen, A. Günther, M. A. Schmidt, K. F. Jensen, and M. G. Bawendi, "A microfabricated gas–liquid segmented flow reactor for high-temperature synthesis: the case of cdse quantum dots," *Angewandte Chemie International Edition*, vol. 44, no. 34, pp. 5447–5451, 2005.

[23] K. Liu, H.-J. Ding, J. Liu, Y. Chen, and X.-Z. Zhao, "Shape-controlled production of biodegradable calcium alginate gel microparticles using a novel microfluidic device," *Langmuir*, vol. 22, no. 22, pp. 9453–9457, 2006.

[24] H. Zhang, E. Tumarkin, R. Peerani, Z. Nie, R. M. A. Sullan, G. C. Walker, and E. Kumacheva, "Microfluidic production of biopolymer microcapsules with controlled morphology," *Journal of the american chemical society*, vol. 128, no. 37, pp. 12205–12210, 2006.

[25] Y. Song, C. S. Kumar, and J. Hormes, "Synthesis of palladium nanoparticles using a continuous flow polymeric micro reactor," *Journal of nanoscience and nanotechnology*, vol. 4, no. 7, pp. 788–793, 2004.

[26] Y. Song, E. Doomes, J. Prindle, R. Tittsworth, J. Hormes, and C. S. R. Kumar, "Investigations into sulfobetaine-stabilized cu nanoparticle formation: toward development of a microfluidic synthesis," *The Journal of Physical Chemistry B*, vol. 109, no. 19, pp. 9330–9338, 2005.

[27] X. Z. Lin, A. D. Terepka, and H. Yang, "Synthesis of silver nanoparticles in a continuous flow tubular microreactor," *Nano letters*, vol. 4, no. 11, pp. 2227–2232, 2004.

[28] J. Köhler, J. Wagner, and J. Albert, "Formation of isolated and clustered au nanoparticles in the presence of polyelectrolyte molecules using a flow-through si chip reactor," *Journal of Materials Chemistry*, vol. 15, no. 19, pp. 1924–1930, 2005.

[29] J. Wagner, T. Kirner, G. Mayer, J. Albert, and J. Köhler, "Generation of metal nanoparticles in a microchannel reactor," *Chemical Engineering Journal*, vol. 101, no. 1-3, pp. 251–260, 2004.

[30] J. Wagner and J. Köhler, "Continuous synthesis of gold nanoparticles in a microreactor," *Nano letters*, vol. 5, no. 4, pp. 685–691, 2005.

[31] E. Y. Erdem, J. C. Cheng, F. M. Doyle, and A. P. Pisano, "Multi-temperature zone, droplet-based microreactor for increased temperature control in nanoparticle synthesis," *small*, vol. 10, no. 6, pp. 1076–1080, 2014.

[32] W.-B. Lee, C.-H. Weng, F.-Y. Cheng, C.-S. Yeh, H.-Y. Lei, and G.-B. Lee, "Biomedical microdevices synthesis of iron oxide nanoparticles using a microfluidic system," *Biomedical microdevices*, vol. 11, no. 1, pp. 161–171, 2009.

[33] D. Pouliquen, H. Perroud, F. Calza, P. Jallet, and J. Le Jeune, "Investigation of the magnetic properties of iron oxide nanoparticles used as contrast agent for mri," *Magnetic resonance in medicine*, vol. 24, no. 1, pp. 75–84, 1992.

[34] J. Dobson, "Magnetic nanoparticles for drug delivery," *Drug development research*, vol. 67, no. 1, pp. 55–60, 2006.

[35] S. Sun and H. Zeng, "Size-controlled synthesis of magnetite nanoparticles," *Journal of the American Chemical Society*, vol. 124, no. 28, pp. 8204–8205, 2002.

[36] S. Krishnadasan, R. Brown, *et al.*, "Intelligent routes to the controlled synthesis of nanoparticles," *Lab on a Chip*, vol. 7, no. 11, pp. 1434–1441, 2007.

[37] M. V. Kutushov, A. A. Kuznetsov, V. I. Filippov, and O. A. Kuznetsov, "New method of biological fluid detoxification based on magnetic adsorbents," in *Scientific and clinical applications of magnetic carriers*, pp. 391–397, Springer, 1997.

[38] L. Babes, B. Denizot, G. Tanguy, J. J. L. Jeune, and P. Jallet, "Synthesis of iron oxide nanoparticles used as mri contrast agents: A parametric study," *Journal of Colloid and Interface Science*, vol. 212, no. 2, pp. 474 – 482, 1999.

[39] J. Park, E. Lee, N.-M. Hwang, M. Kang, S. C. Kim, Y. Hwang, J.-G. Park, H.-J. Noh, J.-Y. Kim, J.-H. Park, and T. Hyeon, "One-nanometer-scale size-controlled synthesis of monodisperse magnetic iron oxide nanoparticles," *Angewandte Chemie International Edition*, vol. 44, no. 19, pp. 2872–2877, 2005.

[40] D. Maity and D. Agrawal, "Synthesis of iron oxide nanoparticles under oxidizing environment and their stabilization in aqueous and non-aqueous media," *Journal of Magnetism and Magnetic Materials*, vol. 308, no. 1, pp. 46 – 55, 2007.

[41] L. Frenz, A. El Harrak, M. Pauly, S. Bégin-Colin, A. D. Griffiths, and J.-C. Baret, "Droplet-based microreactors for the synthesis of magnetic iron oxide nanoparticles," *Angewandte Chemie International Edition*, vol. 47, no. 36, pp. 6817–6820, 2008.

[42] A. Abou Hassan, O. Sandre, V. Cabuil, and P. Tabeling, "Synthesis of iron oxide nanoparticles in a microfluidic device: preliminary results in a coaxial flow millichannel," *Chem. Commun.*, pp. 1783–1785, 2008.

[43] A. Abou-Hassan, R. Bazzi, and V. Cabuil, "Multistep continuous-flow microsynthesis of magnetic and fluorescent -fe2o3@sio2 core/shell nanoparticles," *Angewandte Chemie International Edition*, vol. 48, no. 39, 2009.

[44] "Synthesis of fe3o4@zif-8 magnetic core–shell microspheres and their potential application in a capillary microreactor," *Chemical Engineering Journal*, vol. 228, pp. 398 – 404, 2013.

[45] K. Kumar, A. M. Nightingale, S. H. Krishnadasan, N. Kamaly, M. Wylenzinska-Arridge, K. Zeissler, W. R. Branford, E. Ware, A. J. deMello, and J. C. deMello, "Direct synthesis of dextran-coated superparamagnetic iron oxide nanoparticles in a capillary-based droplet reactor," *J. Mater. Chem.*, vol. 22, pp. 4704–4708, 2012.

[46] M. Baştopçu, A. E. Derinöz, A. C. Yılmaz, and E. Y. Erdem, "Textured surfaces as a new platform for nanoparticle synthesis," *Soft Matter*, vol. 14, pp. 4311–4316, 2018.

[47] H.-Q. Mao, K. Roy, V. L. Troung-Le, K. A. Janes, K. Y. Lin, Y. Wang, J. August, and K. W. Leong, "Chitosan-dna nanoparticles as gene carriers: synthesis, characterization and transfection efficiency," *Journal of Controlled Release*, vol. 70, no. 3, pp. 399 – 421, 2001.

[48] S. Mitra, U. Gaur, P. Ghosh, and A. Maitra, "Tumour targeted delivery of encapsulated dextran–doxorubicin conjugate using chitosan nanoparticles as carrier," *Journal of Controlled Release*, vol. 74, no. 1, pp. 317 – 323, 2001. Proceeding of the International Symposium on Tumor Targeted Delivery Systems.

[49] L. Qi, Z. Xu, X. Jiang, C. Hu, and X. Zou, "Preparation and antibacterial activity of chitosan nanoparticles," *Carbohydrate Research*, vol. 339, no. 16, pp. 2693 – 2700, 2004.

[50] K. A. Janes, M. P. Fresneau, A. Marazuela, A. Fabra, and M. J. Alonso, "Chitosan nanoparticles as delivery systems for doxorubicin," *Journal of Controlled Release*, vol. 73, no. 2, pp. 255 – 267, 2001.

[51] Y. Xu and Y. Du, "Effect of molecular structure of chitosan on protein delivery properties of chitosan nanoparticles," *International Journal of Pharmaceutics*, vol. 250, no. 1, pp. 215 – 226, 2003.

[52] H. Katas and H. O. Alpar, "Development and characterisation of chitosan nanoparticles for sirna delivery," *Journal of Controlled Release*, vol. 115, no. 2, pp. 216 – 225, 2006.

[53] A. Grenha, B. Seijo, and C. Remuñán-López, "Microencapsulated chitosan nanoparticles for lung protein delivery," *European Journal of Pharmaceutical Sciences*, vol. 25, no. 4, pp. 427 – 437, 2005.

[54] F. S. Majedi, M. M. Hasani-Sadrabadi, S. Hojjati Emami, M. A. Shokrgozar, J. J. VanDersarl, E. Dashtimoghadam, A. Bertsch, and P. Renaud, "Microfluidic assisted self-assembly of chitosan based nanoparticles as drug delivery agents," *Lab Chip*, vol. 13, pp. 204–207, 2013.

[55] B. Cetin, M. Asik, and S. D.Taze, "Design and fabrication of a microfluidic device for synthesis of chitosan nanoparticles," *Journal of Nanotechnology in Engineering and Medicine*, vol. 4, pp. 031004–031004–6, 2013.

[56] C.-H. Yang, Y.-S. Lin, K.-S. Huang, Y.-C. Huang, E.-C. Wang, J.-Y. Jhong, and C.-Y. Kuo, "Microfluidic emulsification and sorting assisted preparation of monodisperse chitosan microparticles," *Lab Chip*, vol. 9, pp. 145–150, 2009.

[57] K. H. Lee, S. J. Shin, C.-B. Kim, J. K. Kim, Y. W. Cho, B. G. Chung, and S.-H. Lee, "Microfluidic synthesis of pure chitosan microfibers for bio-artificial liver chip," *Lab Chip*, vol. 10, pp. 1328–1334, 2010.

[58] R. Y. Pelgrift and A. J. Friedman, "Nanotechnology as a therapeutic tool to combat microbial resistance," *Advanced Drug Delivery Reviews*, vol. 65, no. 13, pp. 1803 – 1815, 2013. Nanotechnology and drug resistance.

[59] L.-H. Hung and A. P. Lee, "Microfluidic devices for the synthesis of nanoparticles and biomaterials," *Journal of Medical and Biological Engineering*, vol. 27, no. 1, p. 1, 2007.

[60] H. Wang, X. Li, M. Uehara, Y. Yamaguchi, H. Nakamura, M. Miyazaki, H. Shimizu, and H. Maeda, "Continuous synthesis of cdse–zns composite nanoparticles in a microfluidic reactor," *Chem. Commun.*, pp. 48–49, 2004.

[61] Q. Zhang, J.-J. Xu, Y. Liu, and H.-Y. Chen, "In-situ synthesis of poly(dimethylsiloxane)–gold nanoparticles composite films and its application in microfluidic systems," *Lab Chip*, vol. 8, pp. 352–357, 2008.

[62] C.-H. Yang, L.-S. Wang, S.-Y. Chen, M.-C. Huang, Y.-H. Li, Y.-C. Lin, P.-F. Chen, J.-F. Shaw, and K.-S. Huang, "Microfluidic assisted synthesis of silver nanoparticle–chitosan composite microparticles for antibacterial applications," *International Journal of Pharmaceutics*, vol. 510, no. 2, pp. 493 – 500, 2016. Advanced nano- and bio-materials: a pharmaceutical approach.

[63] D. K. Hwang, D. Dendukuri, and P. S. Doyle, "Microfluidic-based synthesis of non-spherical magnetic hydrogel microparticles," *Lab Chip*, vol. 8, pp. 1640–1647, 2008.

[64] P. M. Valencia, P. A. Basto, L. Zhang, M. Rhee, R. Langer, O. C. Farokhzad, and R. Karnik, "Single-step assembly of homogenous lipid−polymeric and lipid−quantum dot nanoparticles enabled by microfluidic rapid mixing," *ACS Nano*, vol. 4, no. 3, pp. 1671–1679, 2010.

[65] D. Pouliquen, H. Perroud, F. Calza, P. Jallet, and J. J. Le Jeune, "Investigation of the magnetic properties of iron oxide nanoparticles used as contrast agent for mri," *Magnetic Resonance in Medicine*, vol. 24, no. 1, pp. 75–84, 1992.

[66] Y.-X. J. Wang, S. M. Hussain, and G. P. Krestin, "Superparamagnetic iron oxide contrast agents: physicochemical characteristics and applications in mr imaging," *European Radiology*, vol. 11, pp. 2319–2331, Nov 2001.

[67] J. B. Edel, R. Fortt, J. C. demello, and A. J. demello, "Microfluidic routes to the controlled production of nanoparticles," *Chemical Communications*, no. 10, pp. 1136–1137, 2002.

[68] S. Santra, R. Tapec, N. Theodoropoulou, J. Dobson, A. Hebard, and W. Tan, "Synthesis and characterization of silica-coated iron oxide nanoparticles in microemulsion: the effect of nonionic surfactants," *Langmuir*, vol. 17, no. 10, pp. 2900–2906, 2001.

[69] L. Rao, B. Cai, L.-L. Bu, Q.-Q. Liao, S.-S. Guo, X.-Z. Zhao, W.-F. Dong, and W. Liu, "Microfluidic electroporation-facilitated synthesis of erythrocyte membrane-coated magnetic nanoparticles for enhanced imaging-guided cancer therapy," *ACS nano*, vol. 11, no. 4, pp. 3496–3505, 2017.

[70] K. Nagpal, S. K. Singh, and D. N. Mishra, "Chitosan nanoparticles: a promising system in novel drug delivery," *Chemical and Pharmaceutical Bulletin*, vol. 58, no. 11, pp. 1423–1430, 2010.

[71] P. Couvreur, "Nanoparticles in drug delivery: past, present and future," *Advanced drug delivery reviews*, vol. 65, no. 1, pp. 21–23, 2013.

[72] G. Unsoy, S. Yalcin, R. Khodadust, G. Gunduz, and U. Gunduz, "Synthesis optimization and characterization of chitosan-coated iron oxide nanoparticles produced for biomedical applications," *Journal of Nanoparticle Research*, vol. 14, no. 11, p. 964, 2012.

[73] J. Safari and L. Javadian, "Chitosan decorated fe 3 o 4 nanoparticles as a magnetic catalyst in the synthesis of phenytoin derivatives," *RSC Advances*, vol. 4, no. 90, pp. 48973–48979, 2014.

[74] Z. Zarnegar and J. Safari, "Fe 3 o 4@ chitosan nanoparticles: a valuable heterogeneous nanocatalyst for the synthesis of 2, 4, 5-trisubstituted imidazoles," *RSC Advances*, vol. 4, no. 40, pp. 20932–20939, 2014.

[75] Y. He, M. Pei, Y. Du, F. Yu, L. Wang, and W. Guo, "Synthesis, characterization and application of chitosan coated fe 3 o 4 particles as an adsorbent for the removal of furfural from aqueous solution," *RSC Advances*, vol. 4, no. 57, pp. 30352–30357, 2014.

[76] M. Saqib, O. B. Şahinoğlu, and E. Y. Erdem, "Alternating droplet formation by using tapered channel geometry," *Scientific reports*, vol. 8, no. 1, p. 1606, 2018.

[77] X. Niu, S. Gulati, J. B. Edel, and A. J. deMello, "Pillar-induced droplet merging in microfluidic circuits," *Lab Chip*, vol. 8, pp. 1837–1841, 2008.

[78] G. Wei and P. X. Ma, "Structure and properties of nano-hydroxyapatite/polymer composite scaffolds for bone tissue engineering," *Biomaterials*, vol. 25, no. 19, pp. 4749–4757, 2004.

[79] N. Kantharia, S. Naik, S. Apte, M. Kheur, S. Kheur, and B. Kale, "Nano-hydroxyapatite and its contemporary applications," *Journal of Dental Research and Scientific Development*, vol. 1, p. 15, 01 2014.

[80] C. Du, F. Cui, Q. Feng, X. Zhu, and K. De Groot, "Tissue response to nano-hydroxyapatite/collagen composite implants in marrow cavity," *Journal of Biomedical Materials Research: An Official Journal of The Society for Biomaterials, The Japanese Society for Biomaterials, and the Australian Society for Biomaterials*, vol. 42, no. 4, pp. 540–548, 1998.

[81] C. Müller-Mai, S. I. Stupp, C. Voigt, and U. Gross, "Nanoapatite and organoapatite implants in bone: histology and ultrastructure of the interface," *Journal of biomedical materials research*, vol. 29, no. 1, pp. 9–18, 1995.

[82] I. Yamaguchi, K. Tokuchi, H. Fukuzaki, Y. Koyama, K. Takakuda, H. Monma, and J. Tanaka, "Preparation and microstructure analysis of chitosan/hydroxyapatite nanocomposites," *Journal of Biomedical Materials Research: An Official Journal of The Society for Biomaterials, The Japanese Society for Biomaterials, and The Australian Society for Biomaterials and the Korean Society for Biomaterials*, vol. 55, no. 1, pp. 20–27, 2001.

[83] S. Itoh, M. Kikuchi, Y. Koyama, K. Takakuda, K. Shinomiya, and J. Tanaka, "Development of an artificial vertebral body using a novel biomaterial, hydroxyapatite/collagen composite," *Biomaterials*, vol. 23, no. 19, pp. 3919–3926, 2002.

[84] M. Kikuchi, S. Itoh, S. Ichinose, K. Shinomiya, and J. Tanaka, "Self-organization mechanism in a bone-like hydroxyapatite/collagen nanocomposite synthesized in vitro and its biological reaction in vivo," *Biomaterials*, vol. 22, no. 13, pp. 1705–1711, 2001.

[85] K. S. Tenhuisen, R. I. Martin, M. Klimkiewicz, and P. W. Brown, "Formation and properties of a synthetic bone composite: hydroxyapatite–collagen," *Journal of biomedical materials research*, vol. 29, no. 7, pp. 803–810, 1995.

[86] W. Paul and C. P. Sharma, "Porous hydroxyapatite nanoparticles for intestinal delivery of insulin," *Trends Biomater Artif Organs*, vol. 14, pp. 37–38, 2001.

[87] S. Kano, A. Yamazaki, R. Otsuka, M. Ohgaki, M. Akao, and H. Aoki, "Application of hydroxyapatite-sol as drug carrier," *Bio-medical materials and engineering*, vol. 4, no. 4, pp. 283–290, 1994.

[88] S. S. A. Abidi and Q. Murtaza, "Synthesis and characterization of nanohydroxyapatite powder using wet chemical precipitation reaction," *UPB Sci Bull B*, vol. 75, pp. 3–12, 2013.

[89] S. Puajindanetr, "Characterisation and sintering of precipitated hydroxyapatite," *Ph.D. Thesis, Queen Mary and Westfield College London, Great Britain*, 1993.

[90] S. Kehoe, "Calcium phosphates for medical applications," 2008.

[91] J. Liu, X. Ye, H. Wang, M. Zhu, B. Wang, and H. Yan, "The influence of ph and temperature on the morphology of hydroxyapatite synthesized by hydrothermal method," *Ceramics international*, vol. 29, no. 6, pp. 629–633, 2003.

Appendix A

Fabrication

In order to fabricate PDMS based microreactor, SU-8 mold is prepared which serves as master mold for preparing PDMS based devices. SU-8 mold fabrication has been carried out in clean room at UNAM. The detailed procedure for fabrication is listed below.

A.1   Cleaning of the Silicon Wafer

Firstly a 4-inch Silicon wafer is rinsed with acteone and iso-proponal (IPA) to get rid of all organic and inorganic impurities. Then its throughly washed with DI water and dried by blowing nitrogen using nitrogen gun. After that it is placed in oven at 120°C to remove any mositure that may have left on it.

SU-8 mold is prepared using two layers. Base layer which acts as primer and the main layer which holds the pattern.

A.2 Base Layer

SU-8 2005 is used for base layer which serves as adhesive and keeps the pattern intact to the wafer so that the mold can be reused several times.

A.2.1 Spin coating for base layer

Silicon wafer is cooled to room temperature after taking it out of oven. In the meantime spin parameters entered to the spinner.

Table A.1: Spin parameters for base layer coating

Step	Velocity(rpm)	Acceleration (rpm/s)	Time (seconds)
1	500	100	25
2	2500	200	40

Silicon wafer is held placed in chuck and vaccum is turned on to hold the wafer. 4mL of su08 2005 is poured on to wafer and spinner is turned on. After the spin process has been finished, Silcon wafer is removed from the chuck.

A.2.2 Pre-bake for base layer

After spin coating, the wafer is pre baked to remove solvents.

Table A.2: Pre bake for base layer

Step	Temperature (°C)	Time (seconds)
1	65	2
2	95	4
3	65	1

A.2.3   Exposure for base layer

After the pre-bake, Silicon wafer is exposed through a blank mask to cross link the photo resist. Following parameters are used for the exposure.

- Manual top side

- Contact mode = soft contact

- Separation = 100μm

- Mask thickness = 2.3mm

- Sample thickness = 0.5mm

- Resist thickness = 2μm

- Exposure intensity = 120mJ/cm^2

A.2.4   Post-bake for base layer

After the exposure, post bake is done to solidify the photoresist.

Table A.3: Post bake for base layer

Step	Temperature (°C)	Time (seconds)
1	65	1
2	95	3
3	65	1

A.3   Main layer for micro-channel mold

Main layer is fabricated with SU-8 2050 and it contains the pattern.

A.3.1 Spin coating for main layer

Spin parameters for main layer are as follows.

Table A.4: Spin parameters for main layer coating SU-8 2050

Step	Velocity(rpm)	Acceleration (rpm/s)	Time (seconds)
1	500	50	40
2	2200	300	35

Silicon wafer is held placed in chuck and vacuum is turned on to hold the wafer. 4mL of SU-8 2050 is poured on to wafer and spinner is turned on. After the spin process has been finished, Silicon wafer is removed from the chuck.

A.3.2 Pre-bake for main layer

After spin coating, the wafer is pre baked to remove residual solvents.

Table A.5: Pre bake for main layer

Step	Temperature (°C)	Time (seconds)
1	65	3
2	95	8
3	65	2

A.3.3 Exposure for the main layer

After pre-bake, silicon wafer is exposed through a photo-mask to cross-link the photo resist to form channels. Following parameters are used for exposure.

- Manual top side

- Contact mode = soft contact

- Separation = 200μm

- Mask thickness = 2.3mm

- Sample thickness = 0.5mm

- Resist thickness = 100μm

- Exposure intensity = 230mJ/cm^2

A.3.4 Post-bake for main layer

After exposure, post bake is done to solidify the photoresist.

Table A.6: Post bake for main layer

Step	Temperature (°C)	Time (seconds)
1	65	3
2	95	8
3	65	2

A.4 Development of the SU-8 main layer on the Wafer

After hard back, wafer is cooled down to room temperature and then proceeded for development. Su08 developer is added to a petri dish and wafer is immersed in it and constantly agitated for 9 minutes. After 9 minutes, its rinsed with IPA and water and then blow dried with nitrogen.

Appendix B

PDMS Microreactor Preparation Using Soft Lithography

PDMS devices were prepared by using SU-8 master mold fabricated on a silicon wafer .

Firstly, PDMS and curing agent in 10:1 ratio by mass was mixed for 2-3 minutes. Then the mixture was poured on to the silicon wafer with SU-8 mold and degassed using vacuum pump in a closed chamber. Degassing takes approximately 20 minutes. It is made sure there are no bubbles left in the PDMS mixture. After that its baked for 70 minutes at 80°C . When PDMS is solidified, it is cooled down to room temperature and then peeled off from the wafer. Finally that holes are punched for inlets and outlet.

Then PDMS is bonded to a glass slide using oxygen plasma in clean room. PDMS and glass slides are exposed to plasma at 150 W to activate the bonds on surface and increase the surface energy. Then they are pressed together to be bonded. Later sides of the device are sealed using epoxy. Finally that capillary tubing are fitted using epoxy to deliver the reagents.

Appendix C

Nanoparticles size Measurement

C.1 Chitosan coated iron oxide nanoparticles size measurement

Experiment 3.1

Table C.1: Size Measurement for Experiment 3.1

No	Size(nm)	No	Size (nm)
1	7.8125	21	8.72316
2	8.4375	22	6.9147
3	8.4375	23	7.65936
4	7.1875	24	9.99972
5	6.875	25	8.5104
6	6.5625	26	7.23384
7	6.25	27	11.7018
8	7.1875	28	7.02108
9	7.25	29	9.36144
10	7.375	30	8.29764
11	5.625	31	7.23384
12	7.1875	32	8.29764
13	9.375	33	6.80832
14	5.3125	34	8.29764
15	5	35	7.0625
16	6.25	36	6.125
17	8.28125	37	7.0625
18	8.125	38	5.5625
19	5.9375	39	6.139
20	6.5625	40	7.2791

Experiment 3.2

Table C.2: Size Measurement for Experiment 3.2

No	Size(nm)	No	Size (nm)
No	Size(nm)	No	Size (nm)
1	9.27	21	7.64
2	9.85	22	7.06
3	7.82	23	7.22
4	9.27	24	5
5	8.91	25	6.66
6	6.48	26	6.38
7	8.64	27	7.49
8	5.13	28	7.78
9	6.75	29	6.38
10	6.48	30	7.35
11	8.64	31	5.55
12	8.64	32	7.49
13	7.56	33	7.22
14	7.02	34	10.27
15	6.21	35	6.11
16	6.11	36	6.38
17	10.56	37	6.94
18	7.5	38	7.22
19	9.44	39	6.11
20	10.27	40	5.55

Experiment 3.3

Table C.3: Size Measurement for Experiment 3.3

No	Size(nm)	No	Size (nm)
1	9.27	21	7.64
2	9.85	22	7.06
3	7.82	23	7.22
4	9.27	24	5
5	8.91	25	6.66
6	6.48	26	6.38
7	8.64	27	7.49
8	5.13	28	7.78
9	6.75	29	6.38
10	6.48	30	7.35
11	8.64	31	5.55
12	8.64	32	7.49
13	7.56	33	7.22
14	7.02	34	10.27
15	6.21	35	6.11
16	6.11	36	6.38
17	10.56	37	6.94
18	7.5	38	7.22
19	9.44	39	6.11
20	10.27	40	5.55

Standard deviation:

For each experiment, the standard deviation was calculated based on the measurements presented in the respective table using the Equation C.1.

$$\sigma = \sqrt{\frac{1}{N-1} \sum_{i}^{N} (x_i - x_{avg})^2}$$

(C.1)